UC San Diego

UC San Diego Previously Published Works

Title

Reversal of malignant ADAR1 splice isoform switching with Rebecsinib

Permalink

https://escholarship.org/uc/item/69b2s7xm

Journal

Cell Stem Cell, 30(3)

ISSN

1934-5909

Authors

Crews, Leslie A

Ma, Wenxue

Ladel, Luisa

et al.

Publication Date

2023-03-01

DOI

10.1016/j.stem.2023.01.008

Peer reviewed

eScholarship.org Powered by the California Digital Library
University of California

Author Manuscript

Author Manuscript

Author Manuscript

Author Manuscript

HHS Public Access

Author manuscript

Cell Stem Cell. Author manuscript; available in PMC 2024 March 02.

Published in final edited form as:

Cell Stem Cell. 2023 March 02; 30(3): 250–263.e6. doi:10.1016/j.stem.2023.01.008.

Reversal of Malignant ADAR1 Splice Isoform Switching with Rebecsinib

Leslie A. Crews[1,2], **Wenxue Ma**[1], **Luisa Ladel**[1], **Jessica Pham**[1], **Larisa Balaian**[1,2], **S. Kathleen Steel**[1], **Phoebe K. Mondala**[1], **Raymond H. Diep**[1], **Christina N. Wu**[1], **Cayla N. Mason**[1], **Inge van der Werf**[1], **Isabelle Oliver**[1], **Eduardo Reynoso**[1], **Gabriel Pineda**[1], **Thomas Whisenant**[3], **Peggy Wentworth**[1], **James J. La Clair**[4], **Qingfei Jiang**[1], **Michael D. Burkart**[4], **Catriona H.M. Jamieson**[1,2,*]

[1]Department of Medicine, Division of Regenerative Medicine, Sanford Stem Cell Institute, University of California, San Diego, La Jolla, CA, 92037 USA

[2]Moores Cancer Center, University of California, San Diego, La Jolla, CA, 92093 USA

[3]Center for Computational Biology & Bioinformatics (CCBB), Department of Medicine, University of California, San Diego, La Jolla, CA, 92093 USA

[4]Departments of Chemistry and Biochemistry, University of California, San Diego, La Jolla, CA, 92093 USA

Summary

Adenosine deaminase acting on RNA1 (ADAR1) preserves genomic integrity by preventing retroviral integration and retrotransposition during stress responses. However, inflammatory microenvironment-induced ADAR1p110 to p150 splice isoform switching drives cancer stem cell (CSC) generation and therapeutic resistance in 20 malignancies. Previously, predicting and preventing ADAR1p150-mediated malignant RNA editing represented a significant challenge. Thus, we developed lentiviral ADAR1 and splicing reporters for non-invasive detection of splicing-mediated ADAR1 adenosine to inosine (A-to-I) RNA editing activation; a quantitative ADAR1p150 intracellular flow cytometric assay; a selective small molecule inhibitor of

*Lead Contact (cjamieson@health.ucsd.edu).

Author contributions

L.A.C., M.D.B., and C.H.M.J. conceived of the study, and L.A.C., W.M., L.L., J.P., L.B., S.K.S., P.K.M., R.D., C.N.W., C.N.M., I.V.D.W., I.O., E.R., G.P., and Q.J. designed and/or performed experiments and analyzed data. T.W. performed RNA-sequencing and RNA editing analyses and managed all transcriptomics data and deposition, supervised by L.A.C., W.M., Q.J., and C.H.M.J. L.A.C., P.W., J.J.L.C., M.D.B., and C.H.M.J. designed and coordinated pre-IND-enabling toxicokinetic studies with external service vendors, and J.J.L.C. and M.D.B. synthesized and formulated Rebecsinib preparations for all experiments. L.A.C. and C.H.M.J. wrote the manuscript, which was reviewed and edited by all authors. C.H.M.J. supervised all aspects of the project.

Publisher's Disclaimer: This is a PDF file of an unedited manuscript that has been accepted for publication. As a service to our customers we are providing this early version of the manuscript. The manuscript will undergo copyediting, typesetting, and review of the resulting proof before it is published in its final form. Please note that during the production process errors may be discovered which could affect the content, and all legal disclaimers that apply to the journal pertain.

Declaration of Interests

C.H.M.J. is a co-founder of Aspera Biomedicines and Impact Biomedicines, and receives royalties from Forty Seven Inc. M.D.B. is a co-founder of Aspera Biomedicines. C.H.M.J., L.A.C., M.D.B., L.B., P.K.M., C.N.M, R.H.D., J.J.L.C., T.W., I.V.D.W., P.W., and W.M. are named on patents related to this work. All other authors declare no competing interests.

Inclusion and Diversity

We support inclusive, diverse, and equitable conduct of research.

Author Manuscript Author Manuscript Author Manuscript Author Manuscript

splicing-mediated ADAR1 activation, Rebecsinib, which inhibits leukemia stem cell (LSC) self-renewal and prolongs humanized LSC mouse model survival at doses that spare normal hematopoietic stem and progenitor cells (HSPCs); and pre-IND studies showing favorable Rebecsinib toxicokinetic and pharmacodynamic (TK/PD) properties. Together, these results lay the foundation for developing Rebecsinib as a clinical ADAR1p150 antagonist aimed at obviating malignant microenvironment-driven LSC generation.

Graphical Abstract

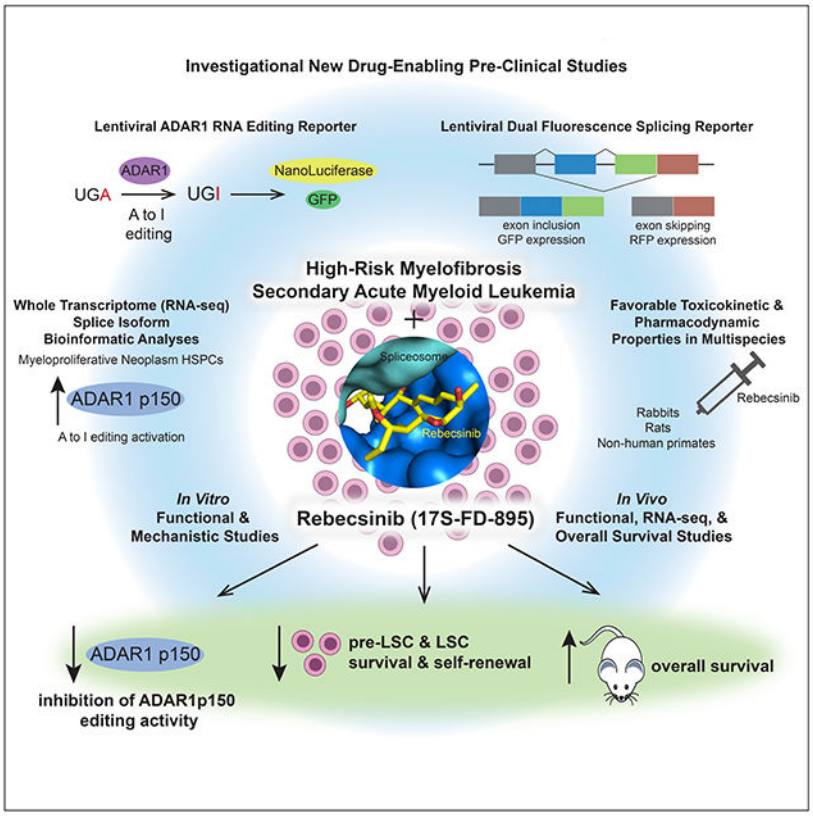

eTOC Blurb

Jamieson and colleagues demonstrate that splicing-mediated activation of the inflammation responsive RNA editase, ADAR1, can be inhibited by Rebecsinib, a selective splicing modulator with favorable safety, pharmacokinetic and pharmacodynamic properties in pre-IND studies. These findings support Rebecsinib development as a potent ADAR1p150 antagonist aimed at preventing leukemia stem cell generation.

Keywords

Myeloproliferative neoplasms; myelofibrosis; secondary AML; leukemia stem cells; splicing; RNA editing; ADAR1; hematopoiesis; cancer stem cells; cancer therapy

Author Manuscript Author Manuscript Author Manuscript Author Manuscript

Introduction

Human innate immune responses against retroviruses are predicated, at least in part, on A-to-I RNA base editing by ADAR1p150.[1] Recently, engineered base editing (BE) strategies have enabled high-throughput functional analyses of cancer-associated single nucleotide variants.[2] Also, antisense oligonucleotide (ASO) mediated A-to-I RNA base editing[3] approaches have been explored as single nucleotide variant correction strategies for inherited disorders that arise from point mutations. However, substantive off-target editing events and ADAR1's capacity to induce malignant transformation and therapeutic resistance in many malignancies have hindered clinical development of ADAR1-mediated BE strategies.[2–4]

Previously, we showed that 1) inflammatory cytokine signalling deregulation in malignant microenvironments drives ADAR1p150 splice isoform overexpression and induces chronic myeloid leukemia (CML) blast crisis transformation, 2) malignant reprogramming of myeloproliferative neoplasm (MPN) hematopoietic stem and progenitor cells (MPN HSPCs) into self-renewing LSCs that drive secondary AML (sAML) therapeutic resistance, and 3) malignant regeneration of multiple myeloma progenitors.[5–9] Since then, human whole transcriptome RNA sequencing (RNA-seq) editome analyses, qRT-PCR detection of edited substrates, and functional therapeutic resistance assays have revealed that ADAR1-mediated A-to-I editing deregulation drives progression of 20 different hematologic malignancies and solid tumor types (reviewed in[10]).[9,11–14] Moreover, ADAR1 activation was shown to induce immune checkpoint blockade (ICB) resistance in cancer.[5,6,9,15–19] While a recent ground-breaking study identified ZPB1 activation of necroptosis with the small molecule curaxin, CBL0137, as an indirect method for inhibiting ADAR1-mediated immune silencing, there remains a pressing need for non-invasive detection and selective inhibition of ADAR1 A-to-I base editing activation, which is a primary driver of CSC generation.[20]

Herein we describe the development of a lentiviral nanoluciferase-GFP (ADAR1 nanoluc-GFP) reporter that enables real-time, non-invasive detection of ADAR1-specific A-to-I RNA editing in human stem and progenitor cells as well as a lentiviral dual fluorescence (GFP/RFP) splicing reporter; and RNA-seq GRCh38-aligned computational bioinformatics platforms for quantifying ADAR1 splice isoform switching in normal human HSPCs, MPN HSPCs and LSCs. In addition, we have developed a flow cytometric assay for quantifying stem and progenitor cell ADAR1p150 protein expression levels and a selective small molecule inhibitor of splicing-mediated ADAR1 activation, Rebecsinib (17S-FD-895). In completed pre-IND studies (PIND 153126), Rebecsinib prevents ADAR1p150-splice isoform expression and malignant A-to-I editing-mediated LSC self-renewal at doses that spare normal HSPCs and are well tolerated in rat, rabbit, and non-human primate pre-IND toxicokinetic, PK and PD studies. Thus, clinical development of Rebecsinib may obviate A-to-I editing driven therapeutic resistance and reduce relapse-related mortality rates in AML and 20 therapeutically recalcitrant, ADAR1p150 overexpressing malignancies.

Author Manuscript Author Manuscript Author Manuscript Author Manuscript

Results

Transcriptomic Detection of ADAR1 Splice Isoform Switching

Inflammatory cytokine-induced splice isoform switching of ADAR1 into the highly active A-to-l editing isoform, ADAR1p150, promotes solid tumor progression and drives high-risk MF hematopoietic progenitor cell (HPC) transformation into LSC.[7–9,15,16,21–25] To determine the impact of ADAR1 splice isoform switching on LSC generation, we performed comparative whole transcriptome sequencing (RNA-seq) analyses of hematopoietic stem cells (HSCs) and HPCs from 1) healthy young and aged bone marrow samples, 2) myeloproliferative neoplasms, including polycythemia vera (PV), essential thrombocythemia (ET) and myelofibrosis (MF), and 3) chronic myeloid leukemia (CML) and AML samples (Table 1). Based on our previous observations that ADAR1-mediated RNA editing and splicing alterations occurs predominantly in the self-renewing $CD34^{+}CD38^{+}Lin^{-}$ HPC population in sAML,[5,8,9,14] we focused on this subpopulation for analysis of RNA editing and splicing changes in MPN pre-LSC and LSC. By evaluating RNA-seq pipelines and data based on GRCh38 (hg38) human genomic assembly,[5] which identifies spliced junctions more reliably than hg19,[26] we observed increased expression of both the standard ADAR1p150 splice isoform, ADAR-202 (GRCh38 transcript ID ENST00000368474.9), and a recently identified ADAR1p150 isoform, ADAR-208 (ENST00000529168.2). The ADAR-208 isoform, which has a truncated 3'UTR that is predicted to prevent microRNA-mediated degradation, was enriched in MPN HPCs compared to normal young and aged bone marrow HPCs, along with the ADAR-202 isoform, while the ADAR-201 isoform was downregulated (Figure 1A). This is in line with our previous observations that changes in ADAR1p150 occur predominantly in the malignant progenitor population and may reflect its central role in disease progression.[9] This observation that a splice isoform switch may favor ADAR1p150 production led to our testing of the capacity of Rebecsinib (17S-FD-895), which binds within the spliceosome core complex (Figure 1B),[27] to induce intron retention and to prevent splicing mediated ADAR1 BE activation (Figure 1C).

A Real-time Lentiviral ADAR1 Reporter for Non-invasive detection of A-to-I RNA Editing

Key challenges in the CSC field include the capacity to reliably predict pre-CSC evolution to self-renewing CSCs and to detect tumor immune microenvironmental (TIME) drivers of dormant CSC maintenance, CSC immune evasion, and CSC therapeutic resistance, such as ADAR1. To date, the standard approach for quantifying ADAR1-mediated A-to-I base editing has relied on complex and cumbersome RNA-seq analyses. Moreover, the cell type and context-dependency of ADAR1 activation combined with the rapid degradation of inosine-containing transcripts, necessitates the development of a non-invasive live-cell detection system to accurately quantify real-time niche-dependent RNA base editing in normal stem cell, pre-CSC and CSC populations. Because lentiviral vectors sustainably integrate into the genomes of dormant stem cells, we chose to develop a lentiviral non-invasive reporter that selectively responds to ADAR1 activation for use in primary normal hematopoietic stem and progenitor cells (HSPCs), MF HPCs and LSCs both in vitro and in vivo.

Author Manuscript Author Manuscript Author Manuscript Author Manuscript

To develop an ADAR1-specific lentiviral A-to-I base editing reporter, we incorporated an ADAR1-specific synthetic nucleic acid sequence[28] into a stem cell promoter-driven (EF1α) pCDH lentiviral vector (Figure S1A) that enables rapid detection of A-to-I editing. Specifically, ADAR1-mediated A-to-I RNA base editing removes a stop codon within the synthetic sequence and induces downstream nanoluciferase and GFP (ADAR1 nanoluc-GFP) expression (Figure 2A). We then overexpressed this vector in combination with a lentiviral ADAR1 overexpression vector that recapitulates endogenous induction of the interferon-responsive ADAR1p150 isoform in human TF-1a AML cells (Figure S1A and B). In contrast to catalytically inactive ADAR1 (E912A) mutant or ADAR2 proteins, the lentiviral ADAR1 nanoluc-GFP reporter showed a dose dependent increase in A-to-I base editing (BE) activity that responded to overexpression of wild-type ADAR1p150, further highlighting the specificity and sensitivity of our BE reporter system (Figures 2B and C). This system represents an important advance over recently described BE reporter and sensor assays that are not selective between ADAR1 and ADAR2 activity,[29,30] due to the functional implications of ADAR1-mediated RNA editing in cancer and stem cell biology. The lentiviral ADAR1 nanoluc-GFP reporter could be detected in human leukemia cells in vitro by confocal fluorescence microscopic detection of GFP (Figure 2D) and by non-invasive (IVIS, Caliper) bioluminescence detection of ADAR1 BE activity in mice engrafted with human leukemia cell lines (K562 and TF-1a) expressing wild-type ADAR1 compared with no transplant and lentiviral pCDH backbone or ADAR1 E912A mutant controls (Figure 2E and Figure S1D). These studies confirmed the specificity and sensitivity of our lentiviral ADAR1 BE reporter both in vitro and in vivo.

Moreover, in a manner that phenocopied ADAR1 shRNA knockdown in a microenvironmentally-responsive TF1a AML cell line, Rebecsinib treatment reduced ADAR1 expression as measured by qRT-PCR, with low levels of AZIN1 transcript editing activity as shown by RNA editing site-specific qPCR (RESSqPCR) detected in shADAR1-transduced cells treated with Rebecsinib compared with vehicle controls (Figure S1E). Moreover, stromal co-cultures assays performed with primary high-risk myelofibrosis (MF) pre-LSC (MF HPCs), which were lentivirally transduced with the lentiviral ADAR1 nano-Luc-GFP reporter, revealed that Rebecsinib treatment significantly reduced ADAR1 RNA editing activity (Figure 2F). Because ADAR1 induces A-to-I intronic editing and upregulation of STAT3 isoforms, which transcriptionally activate ADAR1,[5,8,16] we assessed the effects of Rebecsinib on phospho-STAT3 expression. In keeping with inhibition of ADAR1 base editing activity, Rebecsinib reduced phospho-STAT3 expression, as shown by phospho-STAT3 intracellular flow cytometry (Figure 2G). Together, these studies provided the rationale for testing the high-risk MF HPC and LSC inhibitory efficacy of Rebecsinib in survival and self-renewal assays with multiple primary patient samples (Table 1).

Inhibition of ADAR1p150 Activation Prevents High-risk MF HPC and LSC Maintenance

To quantify ADAR1 protein expression in HSPCs and LSCs, we developed a flow cytometric assay with HSPC and LSC cell surface markers and an ADAR1p150-specific antibody. Compared with vehicle controls, treatment of stromal co-cultures with Rebecsinib (Figure 3A) decreased MF HPC viability commensurate with reduced ADAR1p150 protein expression as detected by intracellular flow cytometry (Figures 3B and C). Both clonogenic

Author Manuscript Author Manuscript Author Manuscript Author Manuscript

survival and replating (self-renewal) assays demonstrated greater sensitivity of secondary AML (sAML) LSC to Rebecsinib than MF HPC or normal cord blood, young bone marrow or aged bone marrow HPCs, independent of splicing factor mutational status in sAML (Figures 3D and E and Figure S1F). In contrast to MF HPC and LSC, no significant differences were detected in normal HSPC and mature hematopoietic progeny exposed to doses of Rebecsinib that decreased LSC survival and self-renewal in co-culture assays (1 μM) compared with DMSO (vehicle) treated controls (Figure S1G). These data provide evidence for a favorable therapeutic index with Rebecsinib.

Splicing Reporter and Splice Isoform Biomarkers of Rebecsinib Response

In addition to testing the effects of Rebecsinib in lentiviral ADAR1 nanoluc-GFP activity assays, we also confirmed its activity using a lentiviral dual fluorescence splicing reporter that shows increased RFP compared with GFP expression upon splicing modulation. The design of this reporter was based on a non-lentiviral reporter construct that was previously tested with Rebecsinib but that was not compatible with use in primary human HSPC.[14,31] Cloning into a lentiviral construct allows confocal microscopic imaging, in vivo imaging of fluorescence (IVIS Caliper), and flow cytometric quantification of splicing activity using the ratio of RFP to GFP signals in primary cells. Rebecsinib impaired $CD34^+$ KG-1a AML cell survival and increased RFP to GFP reporter expression in a dose-dependent manner, with an IC50 dose of approximately 0.1 μM (Figure 4A). In primary patient sample-derived $CD34^+$ MF HPC and LSC short-term culture with Rebecsinib (no stroma), increased exon skipping resulted in elevated expression of pro-apoptotic MCL1-short (S) compared with anti-apoptotic MCL1-long (L) transcripts (expressed as ratios of MCL1-S/L) in all samples treated with 0.1 μM Rebecsinib compared with vehicle (Figures 4B and C). Moreover, Rebecsinib treatment phenocopied ADAR1 shRNA knockdown, with respect to repression of ADAR1 activity, and reduced expression of LSC-associated transcripts, such as CD44v3[13] and MCL1-L. Moreover, ADAR1 shRNA knockdown reduced MCL1-L expression, which is consistent with a previous report involving human cancer cell lines where ADAR1 knockdown attenuates STAT3 activity and subsequent MCL1 transcription.[32] These studies suggest that Rebecsinib inhibits splicing-mediated ADAR1 activation which is a central driver of LSC self-renewal,[5,9,16] and is potentiated by MCL1 splicing modulation.[12]

Rebecsinib Pharmacokinetic, Toxicokinetic and Pharmacodynamic Pre-clinical Studies

To facilitate pharmacodynamic (PD) studies in rats, rabbits and non-human primates (NHP), we developed and validated a panel of functionally relevant species-specific splice isoform biomarker primers to detect responses to Rebecsinib. Based on our current and previous work identifying splice isoform biomarkers of molecular response to splicing modulation,[14,33] the transcripts selected for species-specific primer design included *SF3B* family members and the AML LSC-signature transcript, *PTK2B-202* (Figure S2), along with the pro-survival gene, MCL1, and the LSC self-renewal driver ADAR1p150 (Figures 3 and 4). Three unique human AML cell lines, including KG-1a, MOLM-13 and HL-60, were tested for response to Rebecsinib treatment at a final concentration of 1 μM with significant upregulation of intronic retention of *SF3B* family members (Figure S2A–C), with *SF3B3* demonstrating the most potent and consistent response across all cell lines.

Author Manuscript Author Manuscript Author Manuscript Author Manuscript

Decreased expression of the LSC-related *PTK2B-202* isoform was also observed following treatment with Rebecsinib (Figure S2D). In rat RBL-1 leukemia cells, intron retention in *Sf3b* family members was rapidly induced after treatment with different lots of Rebecsinib (Figures S2E and F). Together, these biomarkers will be used to monitor responses to Rebecsinib treatment in IND-enabling studies.

Pre-IND PD and toxicokinetic (TK) studies (Figure 4D) were enabled by scalable Rebecsinib synthesis[34] and development of an optimized formulation for *in vivo* biodistribution (5% w/v EtOH, 5% w/v Kolliphor HS15 in 0.9% Sodium Chloride). In PK studies, Rebecsinib was detectable in rat (Figure S3A), rabbit (Figure S3B), and non-human primate (NHP) plasma (Figure S3C) following IV bolus administration. In rat TK studies, Rebecsinib was quantifiable up to 1-hour post-dose at 1 mg/kg and up to 4 hours post-dose at 3, 5, and 8 mg/kg (Figure 4E). Rebecsinib T_{max} values were observed by 0.083 hours post-dose at 1 and 5 mg/kg and by 0.167 hours post-dose at 3 and 8 mg/kg. Rebecsinib $T_{1/2}$ values were 0.342, 0.447, 0.313, and 0.530 hours at 1, 3, 5, and 8 mg/kg, respectively (Figure S3A). In rabbit TK studies, plasma $t_{1/2}$ values ranged from 0.12 to 0.89 hours (Figure S3B). Following 3, 10, and 20 mg/kg boluses, Rebecsinib was quantifiable in plasma 1 hour post-dose and could be detected up to 8 hours post-dosing with 40 mg/kg (Figure 4F). In NHP TK studies, peak (C_{max}) and total (AUC_{last}) levels following exposure to Rebecsinib were comparable between male and females at all dose levels (Figure S3C). Following 3, 10, 15, and 20 mg/kg of Rebecsinib, quantifiable plasma concentrations of Rebecsinib were observed through 8 hrs post-dose (Figure 4G). Rebecsinib half-life ($t_{1/2}$) values ranged from 0.62 to 1.1 hours (Figure S3C). While one female NHP in the 20 mg/kg treatment group developed diarrhea, it resolved within 24 hours with no treatment and no sequelae indicative of favorable tolerability.

Pharmacodynamic studies were conducted on peripheral blood mononuclear cells (PBMCs) isolated from NHPs treated with escalating doses of Rebecsinib (3 mg/kg, 10 mg/kg, 15 mg/kg or 20 mg/kg) or a vehicle control and collected at 30 minute and 4 hours post-dose. Splice isoform-specific qRT-PCR demonstrated on-target splicing modulation typified by *MCL1* exon skipping and *SF3B3* intron retention following Rebecsinib dosing (Figure 4H and Figure S2G). Compared with vehicle, *SF3B3* intron retention levels increased at 30 min following single Rebecsinib doses of 3, 10, 15 or 20 mg/kg and were detectable at 4 hours (Figure S2G). Taken together, TK studies show favorable characteristics and PD analyses demonstrate predictable, dose-dependent splicing modulation with Rebecsinib.

Rebecsinib-mediated Inhibition of ADAR1 Splicing Reduces LSC Self-Renewal

To evaluate the inhibitory efficacy of Rebecsinib, we performed *in vivo* humanized LSC mouse model serial transplantation assays, as a gold-standard measurement of self-renewal of the malignant progenitor (pre-LSC and LSC) population, as well as survival assays (Figure 5A).[14] With a twice weekly dosing regimen, there was a significant reduction in sAML LSC burden in the bone marrow, peripheral blood, and spleen of Rebecsinib-treated mice engrafted with splicing factor mutated and unmutated primary AML patient samples (Figure 5B and Figures S4A and B). There was a concomitant increase in the pro-apoptotic

Author Manuscript Author Manuscript Author Manuscript Author Manuscript

MCL1-S isoform expression in human $CD34^+$ cells isolated from the bone marrows of these mice (Figure S4C).

In purified human $CD34^+$ cells derived from Rebecsinib-treated sAML50261 engrafted mice, there was a significant reduction in total ADAR1 RNA expression by qRT-PCR (Figure 5C) as well as LSC-specific splice isoform biomarkers, including *CD44-012* and *PTK2B-202*, compared with vehicle treated controls (Figures S4D and E). Moreover, RNA-seq-based analyses of ADAR1 transcript splicing revealed unique retained intron regions and alternative splice site usage in Rebecsinib-treated samples (Figure S4F). In Rebecsinib-treated sAML50261 engrafted mice, intracellular flow cytometry assays detected significantly decreased ADAR1p150 protein isoform levels in both human HSC and HPC compared with vehicle controls (Figure 5D and Figure S4G). A comprehensive investigation of the molecular changes after in vivo Rebecsinib treatment from our previous datasets [14] revealed a global downregulation of RNA editing activity that occurred in a dose-responsive manner, concomitant with splice isoform switching of MCL1-L to MCL1-S, in mice treated with 5 or 10 mg/kg of Rebecsinib (Figures 5E and F). In comparative *in vivo* studies using fedratinib, a small molecule JAK2 inhibitor that modulates ADAR1 expression by inhibiting its transcriptional activation by STAT3, we found no alteration of MCL1 splicing but, as expected, we observed significantly reduced ADAR1 expression (Figures S4H and I). In contrast, Rebecsinib inhibits both MCL1-L pro-survival transcript expression and ADAR1p150-mediated RNA editing suggesting that it has the capacity to impair LSC survival and self-renewal.

To test this, we performed serial transplantation assays of cells harvested from SAML50261 LSC engrafted mice that were treated intravenously twice weekly for two weeks with Rebecsinib at 10 mg/kg (serial transplant recipients received no further treatment). Flow cytometry analyses of human hematopoietic cell engraftment confirmed that there was a reduced frequency of hematopoietic progenitors ($CD34^+CD38^+Lin^-$) in the spleens of serial transplant recipients of cells isolated from treated mice (Figure S4J and K). Serial transplantation after treatment of a splicing factor mutated sAML (2008-5) engrafted mouse model confirmed that Rebecsinib treatment significantly reduced LSC self-renewal (Figure S4L). In a separate cohort, mice that received $CD34^+$ cells from Rebecsinib-treated splicing factor unmutated sAML 50261 engrafted mice displayed a significant improvement in overall survival, indicative of a significant reduction in LSC self-renewal capacity (Figure 5G). Intriguingly, further molecular analysis of serially transplanted cells harvested from these mice revealed that a less well-characterized interferon-responsive transcript of ADAR1, ADAR-208, which encodes for ADAR1p150 but has a truncated 3'UTR and is lacking a short region of the dsRNA binding domain, shows sustained reductions in expression after serial transplantation compared with ADAR1p110 (Figure 5H and S4M). Thus, reductions in ADAR1p150-mediated RNA editing activity following Rebecsinib treatment correspond with a reversion to a healthy splice isoform expression profile[14] in engrafted human progenitors. Together, these results demonstrate that Rebecsinib reduces both the survival and self-renewal potential of sAML LSC in primary patient-derived splicing factor-mutated and unmutated LSC engraftment models, and promotes improved mouse survival in serial transplantation assays. These results demonstrate that Rebecsinib-

Author Manuscript Author Manuscript Author Manuscript Author Manuscript

mediated inhibition of ADAR1p150 splice isoform expression and activity impairs LSC self-renewal *in vivo*.

Normal Human HSPCs Exhibit Functional Resistance to Rebecsinib

To determine the sensitivity of normal HSPCs to Rebecsinib, human cord blood-derived $CD34^+$ cells were transplanted into $Rag2^{-/-}\gamma c^{-/-}$ mice. After human cell engraftment was established (6 to 12 weeks), mice were treated with Rebecsinib twice-weekly for two weeks at doses equivalent to the maximum doses selected for *in vivo* LSC assays. The frequency of $CD45^+$ hematopoietic cells in bone marrow, peripheral blood, spleen, and thymus were unchanged between vehicle and Rebecsinib-treated groups that received a dose of 10 mg/kg (Figure S5A). Moreover, flow cytometric analyses showed no significant reduction in human $CD3^+$ T cells in thymus or peripheral blood samples or in $CD19^+$ B cells in the bone marrow, peripheral blood, or spleen of mice treated with Rebecsinib compared with vehicle controls (Figure S5B and C). In mice treated with 20 mg/kg of Rebecsinib, there was a reduction in human $CD45^+$ and CD19+ cells in the peripheral blood cell engraftment but not in the bone marrow or spleen (Figures S5A and C). Thus, a dose of 10 mg/kg in mice is sufficient to reduce *in vivo* sAML LSC burden while sparing normal HSPC development. In addition, no evidence of Rebecsinib-related systemic toxicity was observed after 2 weeks of dosing at 10 or 20 mg/kg in this humanized *in vivo* model of normal HSPC development.

After completion of treatment and engraftment analyses of *in vivo* normal HSPC assays, total human hematopoietic cells ($CD45^+$) were selected for splice biomarker analyses to determine sensitivity of normal human hematopoietic cells to Rebecsinib compared with sAML LSC. These analyses showed no changes in *SF3B3* intron retention in the bone marrow but a trend toward changes in the spleen that were not statistically significant (Figures S5D and E). Together, our humanized mouse model assays combined with our splice isoform biomarker system confirms a functional and molecular therapeutic index for Rebecsinib, whereby sAML LSC are significantly more sensitive to splicing modulation than normal HSPCs and their progeny.

Sensitive Detection of ADAR1 Activity in Primary Human Cells *In Vivo*

To further test the utility of the ADAR1 nanoluc-GFP reporter for *in vivo* detection of endogenous ADAR1 activity, primary human aged normal bone marrow $CD34^+$ cells were transduced with the reporter vector and transplanted into immunocompromised mice. ADAR1 activity was detected by live animal bioluminescence imaging and corresponded with human cell engraftment detection by flow cytometry (Figure S5F–H). Moreover, treatment of this normal aged HSPC *in vivo* model with Rebecsinib at 10 mg/kg confirmed that healthy human hematopoietic cells tolerate splicing modulation (Figure S5G and H), with no loss of human HSPC engraftment or mature T or B cell maturation (Figure S5I–K). In comparison to cord blood transplantation models, the frequency of normal CD34+ cells appeared to be increased in the bone marrow of Rebecsinib-treated animals (Figure S5I). This suggests that Rebecsinib spares normal HSPC survival and retention in the bone marrow niche, which is the subject of ongoing mechanistic studies. Together, these results further support a favorable therapeutic index of Rebecsinib that has been observed in comprehensive *in vitro* and *in vivo* IND-enabling studies.

Author Manuscript Author Manuscript Author Manuscript Author Manuscript

Discussion

In sAML, 5-year survival rates of only 26%, are fueled, at least in part, by therapy resistant LSC survival and self-renewal.[35] Over 50% of patients succumb to AML in the first year (10,590 deaths out of 21,380 new cases in 2017[36]) and mortality rates have remained similar over four decades thereby underscoring the pressing unmet need for selective LSC inhibitors. Despite advances in molecularly targeted therapy, morbidity and mortality rates also remain elevated for patients with high-risk MF.[37] Inflammatory microenvironment-induced adenosine-to-inosine (A-to-I) hyper-editing by ADAR1 has been linked to therapeutic resistance in sAML, MF, chronic myeloid leukemia, multiple myeloma and 14 different solid tumor types.[5,7–9,15,16,23] Also, recent studies show that splicing deregulation drives therapeutic resistance and that inflammatory cytokine induced A-to-I RNA editing introduces novel splice acceptor sites, such as in STAT3, which promote LSC generation.[14,38–40] Previously, we showed that LSC splicing deregulation was associated with increased sensitivity to the splicing modulator, 17S-FD-895 (Rebecsinib). However, a mechanistic link between A-to-I editing activation by ADAR1 and splicing deregulation had not been established.

To determine if niche-dependent splicing deregulation drives ADAR1 activation, we developed sensitive lentiviral ADAR1 nanoluciferase GFP and lentiviral dual fluorescence splicing reporters that enable non-invasive imaging, confocal fluorescence microscopic detection and flow cytometric quantification of ADAR1 activation and splicing deregulation in selective microenvironments. In addition, we developed ADAR1 shRNA knockdown and ADAR1p150 overexpression vectors for use in normal HSPC, MF HPC and LSC human SCF, IL-3 and GM-CSF secreting stromal co-cultures and humanized mouse model systems. By demonstrating that genetic inhibition of ADAR1 expression with lentiviral shRNA knockdown vectors phenocopies pharmacologic splicing inhibition with Rebecsinib, we discovered that A-to-I hyper-editing is predicated on ADAR1 splice isoform switching favoring ADAR1p150 over ADAR1p110.

Moreover, we found that ADAR1p150 inhibition with Rebecsinib was well tolerated at doses that eradicated LSC and spared normal HSPC. As a result of ADAR1 induced self-renewal dependency, Rebecsinib treatment inhibited sAML LSC replating and serial transplantation and enhanced survival of humanized sAML mouse models commensurate with dose-dependent changes in ADAR1p150 transcript and protein expression as well as decreased A-to-I editing activity. These in vitro and in vivo studies provided a mechanistic link between microenvironmentally-driven splicing deregulation and ADAR1-mediated A-to-I editing activation in LSC in sAML and potentially in other ADAR1-activated malignancies.[24] In addition to preventing ADAR1 transcript processing, Rebecsinib reduces LSC-enriched anti-apoptotic transcripts, including MCL1-L, BCL-XL, and BCL-2, and induces marked intron retention in splicing factor gene products, such as *SF3B1* and *SF3B3*, which form part of the splicing modulator binding pocket.

In multi-species (rat, rabbit, NHP) pre-IND studies, Rebecsinib was well tolerated and induced dose-dependent increases in splicing modulation. With a clinically tractable formulation, Rebecsinib showed predictable pharmacokinetic and pharmacological (PK/PD)

Author Manuscript Author Manuscript Author Manuscript Author Manuscript

properties combined with favorable bioavailability and stability thereby enabling twice-weekly intravenous dosing regimens with no evidence of systemic toxicity.

The high likelihood of clinical feasibility with Rebecsinib is based on extensive pre-clinical studies showing chemical stability, toxicokinetic safety, favorable pharmacokinetic and pharmacodynamic properties, and highly efficacious human MF HPC and LSC-targeting capacity in splicing factor-mutated and unmutated humanized models of sAML. While one chemically distinct splicing modulator, H3B-8800, completed Phase 1 clinical trials for hematologic malignancies resulted in red blood transfusion independence in some patients, its efficacy was dependent on SRSF2 mutations and it was not sufficiently potent to induce durable remissions.[41] Another splicing modulator, E7107, induced reversible optic neuritis in 2 of 26 patients with solid tumors,[42,43] which was related to compound instability[44] and resulted in early clinical trial discontinuation. In contrast, Rebecsinib has a favorable potency profile and therapeutic index compared to other splicing modulators. Overall, this study lays the foundation for clinical development of Rebecsinib as an ADAR1 self-renewal pathway inhibitor aimed at obviating LSC driven therapeutic resistance and relapse in patients with high-risk MF and sAML and potentially for other malignancies that resist immune checkpoint blockade as a result of ADAR1-mediated immune silencing.[19]

Limitations of the Study

As a potent first-in-class ADAR1 inhibitor, Rebecsinib decreases RNA editing by inhibiting ADAR1 splicing into the most active editase, ADAR1p150. While active in high-risk MF HPC and LSC, a limitation of the current study is that we did not examine the dependence of solid tumor CSC self-renewal on splicing mediated ADAR1 activation and sensitivity to Rebecsinib-mediated ADAR1 splicing inhibition. For future IND enabling studies with Rebecsinib, which are beyond the scope of this completed pre-IND proof-of-concept study, we have developed lentiviral ADAR1 reporter expressing tumor organoid-containing nanobioreactors that enable niche-dependent detection of A-to-I editing activation and humanized CSC ADAR1 reporter models. The capacity of Rebecsinib to potently inhibit malignant A-to-I editing may enhance the spectrum of therapeutically sensitive malignancies to include 14 solid tumor types that activate ADAR1.[41]

STAR Methods

RESOURCE AVAILABILITY

Lead Contact—Further information and requests for resources and reagents should be directed to and will be fulfilled by the lead contact, Catriona Jamieson (cjamieson@health.ucsd.edu).

Materials Availability—All unique/stable reagents generated in this study are available from the Lead Contact with a completed Materials Transfer Agreement.

Data and Code Availability

- Whole transcriptome RNA-seq data have been deposited at the database of Genotypes and Phenotypes (dbGaP) at NIH. Accession numbers are listed in the

Author Manuscript Author Manuscript Author Manuscript Author Manuscript

key resources table. Any additional information required to reanalyze the data reported in this paper is available from the lead contact upon request.

- Original code and RNA splicing and editing analysis methods are publicly available via github repository. Links and the DOI are provided in the key resources table.

EXPERIMENTAL MODEL AND SUBJECT DETAILS

In vivo Mouse Studies—All mouse studies were completed in accordance with the University Laboratory Animal Resources and Institutional Animal Care and Use Committee of the University of California (IACUC) regulations. Rag2$^{-/-}\gamma c^{-/-}$ mice and NSG-SGM3 mice (Jackson Laboratories, Bar Harbor, ME) mice were bred and maintained in the Sanford Consortium vivarium according to IACUC-approved protocols. Rag2$^{-/-}\gamma c^{-/-}$ mice exhibit T cell, B cell, and NK cell immunodeficiencies that make them effective transplant hosts for human immune cells. NSG-SGM3 mice produce 2-4ng/mL serum levels of human SCF, GM-CSF, and IL-3, which supports the engraftment of myeloid and lymphoid cells. Animals were housed in groups. Mice were randomly assigned to experimental groups based on engraftment levels (equivalent average peripheral blood engraftment levels were present in vehicle and treatment groups prior to initiation of treatment).

Animals Used in Pre-clinical Toxicokinetic (TK) Studies—Single-dose TK studies were performed in Sprague Dawley rats (Charles River Labs, South San Francisco, CA), New Zealand white rabbits (BASi/Inotiv, West Lafayette, IN), and cynomolgus monkeys (BASi/Inotiv).

Human Subjects—Primary patient samples were obtained from consenting patients at the University of California in accordance with a UC San Diego human research protection program Institutional Review Board (IRB)-approved protocol (#131550). The IRB reviewed this protocol and found that it meets the requirements as stated in 45 CFR 46.404 and 21 CFR 50.51. Human cord blood and normal aged-match samples were purchased as purified CD34^{+} cells (AllCells).

Stromal Co-Culture Assays—Primary patient samples and normal bone marrow controls used for functional assays are described in Table 1. Human HS5 and HS27a[45] or mouse bone marrow cells lines SL (hSCF and hIL3) and M2 (hIL3 and hG-CSF) were irradiated and then mixed at a ratio of 1:1 and incubated overnight for attachment. To establish co-cultures, 10,000-15,000 CD34^{+} cells were added to SLM2 stroma in 1 ml of Myelocult H5100 (STEMCELL Technologies, Vancouver, Canada). Rebecsinib or DMSO control was added at the initiation of co-culture at indicated concentrations. After one week, cells that were both attached to stroma and floating were collected, resuspended in fresh media and plated in methylcellulose (MC) H4330 (STEMCELL Technologies) in triplicate. After 2 weeks primary colonies (more than 40 cells) were counted and individual multilineage colonies were plucked, cells resuspended, and re-plated again in fresh MC. Secondary colonies were counted after another 14 days. Basal colony formation of untreated cells was considered to be 100% and results are presented as % of change.

Author Manuscript Author Manuscript Author Manuscript Author Manuscript

In vitro Culture of Cell Lines—The following cell lines were used for *in vitro* lentiviral reporter assays and biomarker development: human KG-1a cells (AML cells derived from a 59 y/o male, cultured in Iscove's Modified Dulbecco's Medium, Catalog No. 30-2005, 20% fetal bovine serum), human K562 cells (blast crisis chronic myeloid leukemia cells isolated from a 53 y/o female, cultured in Iscove's Modified Dulbecco's Medium, Catalog No. 30-2005, 10% fetal bovine serum), human TF-1a cells (erythroleukemia cells isolated from a 35 y/o male, cultured in RPMI-1640 Medium, ATCC 30-2001, 10% fetal bovine serum), human MOLM-13 (sAML cells isolated from a 20 y/o male, cultured in RPMI-1640 Medium, ATCC 30-2001, 10% fetal bovine serum), human HL-60 cells (acute promyelocytic leukemia cells isolated from a 36 y/o female, cultured in Iscove's Modified Dulbecco's Medium, Catalog No. 30-2005, 20% fetal bovine serum), 293T cells (human kidney epithelial cells from human fetus, cultured in Dulbecco's Modified Eagle's Medium (DMEM) (ATCC 30-2002, 10% fetal bovine serum), and rat RBL-1 cells (leukemia cells isolated from the Wistar strain, cultured in Eagle's Minimum Essential Medium, Catalog No. 30-2003, 10% fetal bovine serum). All cell lines, with the exception of MOLM-13 cells, were obtained from the American Type Culture Collections (ATCC, Manassas, VA) and cultured at 37°C 5% CO_2, and monitored routinely for cell line identity by flow cytometry and for culture integrity by mycoplasma screening. MOLM-13 cells were generously provided by Dr. Dennis Carson (UC San Diego).

METHOD DETAILS

Primary Samples, Whole Transcriptome RNA-sequencing, RNA Editing, and Splice Isoform Analyses—Primary peripheral blood or bone marrow samples from patients with MPNs (n=6 PV, n=2 ET, n=24 MF, n=5 CML) or AML (n=12), along with non-MPN bone marrow controls (n=24) were FACS-purified to isolate live HSC ($CD34^+CD38^-Lin^-$) and HPC ($CD34^+CD38^+Lin^-$) populations, as previously described.[5,14,16] Cells were lysed in RNA extraction buffer and total RNA was extracted using RNeasy micro extraction kits (QIAGEN, Germantown, MD). RNA samples were evaluated for quality. Samples with RNA integrity (RIN) values >7 were processed for whole transcriptome RNA-sequencing (The Scripps Research Institute Next Generation Sequencing Core) on Illumina HiSeq platforms.

RNA-Seq was performed on Illumina's NextSeq 500 sequencer with 150bp paired-end reads. Transcript quantification was performed as previously described.[5] Briefly, sequencing data were de-multiplexed and output as fastq files using Illumina's bcl2fastq (v2.17). Quality control of the raw fastq files was performed using the software tool FastQC.[46] Sequencing reads were aligned to the human genome (hg38) using the STAR v2.5.1a aligner.[47] Read and transcript quantification was performed with RSEM[48] v1.3.0 and GENCODE annotation (genocode.v19.annotation.gtf). The R BioConductor packages edgeR[49] and limma[50] were used to implement the limma-voom[51] method for normalization of transcript levels and calculation of log transformed counts per million (logCPM). For sashimi plots, the .bam alignment files generated with the STAR aligner were input in the Integrated Genomics Viewer (IGV v2.12, https://software.broadinstitute.org/software/igv/). The viewer was navigated to the specific ADAR1 region of interest and a sashimi plot was generated

Author Manuscript Author Manuscript Author Manuscript Author Manuscript

with base level coverage represented by individual bars and junction level coverage represented by arcs.

For RNA editing analyses of whole transcriptome sequencing data, previous datasets were utilized from $CD34^+$ cells isolated from the spleens of SAML50261-engrafted mice treated once weekly with Rebecsinib in a dose-response assay (5 or 10 mg/kg),[14] along with $CD34^+$ cells harvested from mice that were serially transplanted with CD34+ cells from SAML50261-engrafted mice that had been treated twice weekly with Rebecsinib at 10 mg/kg (no further treatment was delivered to serial transplant recipients). Due to limiting number of cells remaining after treatment, cells were pooled from n=4 to 5 mice per condition for sequencing. RNA editing analysis was performed as previously described.[5] Additional analysis code and documentation for the computational analyses are available through Github: https://github.com/ucsd-ccbb/MPN_atlas_methods.

Lentiviral RNA Splicing and ADAR1 Editing Reporters—To enable real-time, live cell RNA splicing and editing quantification detection, lentiviral dual fluorescence RNA splicing and ADAR1-dependent RNA editing vectors were designed and tested for activity in human leukemia cell lines. To assess ADAR1-dependent editing, a lentiviral reporter was constructed to measure activity by fluorescence and or luminescence. The construct contains a synthetic ADAR1-specific nucleic acid sequence[28] ("Herbert sequence") that was cloned into a pCDH (System Biosciences) backbone containing an EF1α promoter and T2A sequence for co-expression of nanoluciferase and COP-GFP. The Herbert sequence precedes a stop codon, UGA, which lies upstream of NanoLuc T2A copGFP. Following A-to-I editing, this stop codon is removed, resulting in downstream nanoluciferase and COP-GFP expression. The ADAR1-dependent RNA editing reporter vector was validated in 293T cells via co-transfection with various ADAR-overexpression vectors including ADAR1-FLAG wildtype, ADAR1-FLAG E912A (editing-deficient), ADAR2-FLAG and corresponding backbone. ADAR-overexpression plasmids were transfected at 3 concentrations (0.1 μg, 0.3 μg, 1.0 μg) to demonstrate the sensitivity of ADAR1-dependent editing. Cells were collected for western blot to confirm ADAR overexpression using anti-FLAG M2 antibody (Sigma F3165). Reporter activity was measured by luminescence using Nano-Glo Luciferase Assay System (Promega).

For generation of stably transduced splicing reporter cell lines, a previously described splicing reporter construct[31] was cloned into a lentiviral vector backbone.[52] KG-1a cells were transduced with the dual-fluorescent lentiviral splicing reporter vector, treated with various concentrations of Rebecsinib (3-fold serial dilutions from 3 μM to 4 nM) for 24 hr, washed followed by DAPI staining, and analyzed by flow cytometry for cell viability and RFP/GFP fluorescence intensity. Results were from duplicate wells of each condition. Viability of cells treated with DMSO (0.5% final concentration) was set as 100%. Nonlinear regression curve fit analysis was carried out using Prism software (GraphPad) to determine EC_{50} values for viability and mean fluorescence intensity (MFI) of RFP and GFP.

In Vitro Cell Line Treatments and Analyses—For lentivirus-mediated knockdown of human ADAR1 in ADAR1 activation and RNA editing biomarker studies of the nanoluc-GFP reporter and endogenous transcripts, human leukemia cells were stably

Author Manuscript Author Manuscript Author Manuscript Author Manuscript

transduced with the lentiviral shRNA vectors targeting ADAR1 (shADAR1) or scrambled control (shCtrl) to ablate endogenous ADAR1 expression. The shRNA plasmids targeting ADAR1 (shADAR1) as well as the scrambled control (shCtrl) were purchased from VectorBuilder (Chicago, IL) (shCtrl: CCTAAGGTTAAGTCGCCCTCG and shADAR1: CCGGACCTCCTCACGAGCCCAAGTTCGTTTACCAAGCAAAA). Human wild-type or catalytically inactive (E912A) mutant vectors were also used to selectively express ADAR1p150 in some experiments. Viral titers were assessed by qRT-PCR and transduction efficiency was tested in 293T cells. 100,000 TF-1a cells stably transduced with the same lentiviral shCtrl (TF-1a shCtrl) and shADAR1 (TF-1a shADAR1) vectors were plated (n=4) and treated with interferon-α or 0.1 μM Rebecsinib or DMSO control for 4 hours.

For ADAR1 protein isoform and STAT3 phosphorylation analyses in cell lines, western blots were performed as previously described.[5,8,16] Blots were probed with antibodies against ADAR1p150 (Abcam ab126745) and pan-ADAR1 (detects ADAR1p150 and p110, Cell Signaling D7E2M), along with total STAT3, phosphorylated STAT3 (Y705 D3A7, Cell Signaling), and GAPDH as a loading control (Key Resources Table).

Stromal Co-cultures and ADAR1 Reporter Assays—Human HS5 and HS27a[45] or mouse bone marrow cells lines SL (hSCF and hIL3) and M2 (hIL3 and hG-CSF) were irradiated and then mixed at a ratio of 1:1 and incubated overnight for attachment. $CD34^+$ were selected from high-risk MF and sAML primary samples using magnetic beads (Miltenyi Biotec, Germany). As a control, $CD34^+$ cells from aged normal bone marrow (aNBM), young normal BM (yNBM) and cord blood (All Cells Inc, Alameda, CA) mononuclear cells were utilized. To establish co-cultures, 10,000-15,000 $CD34^+$ cells were added to SLM2 stroma in 1 ml of Myelocult H5100 (STEMCELL Technologies, Vancouver, Canada). Rebecsinib or DMSO control were added at the initiation of co-culture at indicated concentrations. After one week, cells that were both attached to stroma and floating were collected, resuspended in fresh media and plated in methylcellulose (MC) H4330 (STEMCELL Technologies) in triplicate. After 2 weeks primary colonies (more than 40 cells) were counted and individual multilineage colonies were plucked, cells resuspended and re-plated again in fresh MC. Secondary colonies were counted after another 14 days. Basal colony formation of untreated cells was considered to be 100% and results are presented as % of change.

For nanoluciferase RNA editing activity assays, $CD34^+$ selected cells from primary high-risk MF samples were lentivirally transduced with ADAR1 nanoluc-GFP reporter for 48 hr, followed by treatment with DMSO or Rebecsinib in stromal co-culture for 72 hr. Luminescence reporter activity was measured in 10,000 cells by Nano-Glo Luciferase Assay and values were normalized to cell viability. Cell viability was measured in 10,000 cells by CellTiter-Glo Luciferase Assay (Promega). A pilot *in vivo* reporter assay was also performed using TF-1a cells that were stably transduced with the ADAR1 nanoluc-GFP reporter. For this purpose, cells were co-transduced with lentiviral vectors expressing ADAR1-targeted shRNA (to knock down endogenous wild-type ADAR1) and wild-type or catalytically inactive mutant (E912A) exogenous human ADAR1p150. Cells were transplanted into neonatal $Rag2^{-/-}\gamma c^{-/-}$ mice (70,000 cells per mouse), and animals were

Author Manuscript Author Manuscript Author Manuscript Author Manuscript

imaged 4 weeks after transplant on the IVIS 200, as previously described.[7,9] Human cell engraftment was also confirmed in the peripheral blood in the same week as imaging.

For normal bone marrow control survival and differentiation assays, $CD34^+$ cells from aged bone marrow samples were plated into StemPro media (ThermoFisher, Carlsbad, CA) and treated with Rebecsinib for 72 hr. Samples were analyzed by flow cytometry using antibodies for total hematopoietic cells (CD45 APC; Life Technologies cat#MHCD4505, 1:50), T cells (CD3 FITC; BioLegend cat#300306, 1:20), monocytes (CD14 PerCP-Cy5.5; BD Pharmingen cat#550787, 3:100) and B cells (CD19 PE; BioLegend cat#302208, 1:50).

Splice Isoform Specific Quantitative RT-PCR—For quantitative analysis of splice isoform expression, RNA editing rates, and whole gene expression by qRT-PCR, cells or tissue fragments were harvested in RNA lysis buffer and total RNA was extracted using RNeasy mini or micro extraction kits (QIAGEN, Germantown, MD) following the manufacturer's protocol including a DNase incubation step to digest any trace genomic DNA present. Levels of ADAR1 variants and LSC-specific transcripts were quantified by qRT-PCR as previously described.[14] RNA-editing site-specific qRT-PCR (RESSqPCR) was performed for variants in AZIN1 transcripts.[53] Additional species-specific primers were also designed to quantify intron retention rates in cells treated with Rebecsinib as a biomarker of response to RNA splicing modulation. Specifically, for the two-step SYBR-green based assays, as previously described,[7,14,53] 100-1000 ng of RNA were subjected to cDNA synthesis using the Superscript III (ThermoFisher Scientific) kit followed by qRT-PCR using SYBR GreenER (ThermoFisher Scientific) master mix according to the manufacturer's recommended procedures. qRT-PCR was performed using SYBR GreenER Super Mix (Life Technologies) on BioRad iQ5, C1000 Touch, or BioRad CFX384 instruments. Human splice isoform-specific, RNA editing site-specific qPCR (RESSqPCR),[53] and whole gene primers used are listed in Table S1. Primer sets that have not been previously published were designed and tested for efficiency followed by analyses in samples exposed to Rebecsinib, with species-specific HPRT primers used as controls. Samples with Ct<35 for the species-specific reference gene, HPRT, were included in analyses. Relative mRNA expression values were calculated using the $2^{-\Delta CT}$ method, with normalization to untreated or vehicle-treated controls.[54]

For multi-species biomarker development and transcript variant-specific qRT-PCR experiments, human AML cell lines KG-1a, MOLM-13, and HL-60, and rat leukemia cells RBL-1 were grown to confluence and treated with 1 μM Rebecsinib for 4 hr. Cells were collected and lysed in Qiagen RNA lysis buffer, and analyzed using the species-specific primers and qRT-PCR procedures described above.

Intracellular ADAR1p150 and Phospho-STAT3 Flow Cytometric Analyses— Flow cytometry for stem and progenitor cell surface antibody staining was performed as previously described.[14] For phospho-flow, a subset of samples was fixed and permeabilized, then blocked and stained with APC-conjugated ADAR1p150 antibody (cat ab269444, 1:25) and pSTAT3 APC (cat 17-9033-42, 1:10) (Key Resources Table). Fractions were analyzed with the BD LSR Fortessa (Sanford Consortium for Regenerative Medicine Stem Cell Core) and FlowJo software (TreeStar, Ashland, OR).

Author Manuscript Author Manuscript Author Manuscript Author Manuscript

Humanized LSC Mouse Model Assays and Human HSPC Therapeutic Index Studies—In humanized mouse models, sAML cells ($CD34^+$) from two unique primate patient samples that were splicing factor mutated or unmutated were utilized, including SAML50261 and SAML20085.[14] For *in vivo* efficacy and therapeutic index studies, sAML $CD34^+$ cells, or normal human cord blood-derived or aged bone marrow-derived HSPCs ($CD34^+$), were transplanted (50,000-200,000 cells per mouse) intrahepatically into neonatal $Rag2^{-/-}\gamma c^{-/-}$ mice, or intravenously into adult NSG-SGM3 mice (Jackson Laboratories, Bar Harbor, ME). A subset of experiments was performed with normal aged bone marrow cells that were transduced with the lentiviral ADAR1 nanoluc-GFP reporter vector prior to transplant. For transplantation into adult mice, animals were irradiated with ^{137}Cs at a dose of 150 cGy 24 hr before IV transplantation. After engraftment levels reached >1% human $CD45^+$ hematopoietic cells in the peripheral blood, animals were distributed among treatment groups for treatment with Rebecsinib or vehicle control essentially as previously described, with an increased dosing regimen of twice weekly (versus once weekly in prior studies)[14] and an optimized *in vivo* formulation (2% w/w EtOH, 5% w/v Kolliphor HS 15 in 0.9% saline). For animals that received transplants of cells transduced with the lentiviral ADAR1 nanoluc-GFP reporter, mice were imaged 15 weeks after transplant on the IVIS 200, as previously described.[7,9] Following treatment with Rebecsinib (five intravenous doses total over a two-week period), hematopoietic tissues (peripheral blood, bone marrow, spleens) were collected and analyzed by flow cytometry as previously described.[14] For splice isoform-specific qRT-PCR or RNA-seq analyses on cells from *in vivo* studies, human $CD34^+$ LSC from bone marrows and spleens of engrafted mice were isolated by magnetic bead separation (Miltenyi Biotec).

Additional aliquots of CD34+ cells from bone marrow and/or spleens of treated and control animals were used for serial transplantation assays after Rebecsinib treatment, including engraftment studies and overall survival assays. In a separate cohort of animals, mice were treated with Fedratinib for two weeks (twice daily oral delivery at 60 mg/kg) as a positive control for modulation of ADAR1 expression and activity.[8]

Pre-clinical Toxicokinetic (TK), Pharmacokinetic and Pharmacodynamic (PD) Studies—Single-dose TK studies were performed in Sprague Dawley rats (Charles River Labs, South San Francisco, CA), New Zealand white rabbits (BASi/Inotiv, West Lafayette, IN), and cynomolgus monkeys (BASi/Inotiv). Rat and rabbit studies included toxicology analyses, quantification of plasma levels of Rebecsinib, and necropsies to evaluate organ integrity after treatment. For NHP studies, health and ophthalmological evaluations were performed before and after dosing with Rebecsinib, and blood samples were collected for quantification of plasma levels of Rebecsinib and biomarker studies in PBMCs from treated and control animals. All monkeys were returned to the animal colony after the end of the observation period. Toxicokinetic values including mean plasma concentrations and $t_{1/2}$ values were calculated according to CRO-approved protocols (Charles River and BASi).

QUANTIFICATION AND STATISTICAL ANALYSIS

Statistical Analyses—For ADAR1 and splicing reporter assays, qRT-PCR analyses, and flow cytometry, data were analyzed using Microsoft Excel and plotted for graph preparation

Author Manuscript Author Manuscript Author Manuscript Author Manuscript

and statistical analyses in Prism GraphPad (San Diego, CA). Differences were assessed by unpaired or paired Student's t-tests, as indicated in the figure legends, and considered statistically significant for p values of <0.05. For stromal co-culture assays and multiple group comparisons, data (means) for summarized sAML, MF or healthy control samples were calculated and graphed. Error bars indicate the SD or SEM, as indicated in individual figure legends. Student's t-test and one-way ANOVA statistical analyses were performed using Prism GraphPad and comparisons described in each figure legend.

Supplementary Material

Refer to Web version on PubMed Central for supplementary material.

Acknowledgements

We would like to thank our funding agencies for their vital support, including NIH/NCI R01CA205944, NIH/NIDDK R01DK114468-01, NIH/NCI 2P30CA023100-28, CIRM TRAN1-10540 for Rebecsinib pre-IND studies, MPN Research Foundation, LLS Blood Cancer Discoveries for biomarker analysis, NASA NRA NNJ13ZBG001N, and NIH/NCATS UL1TR001442. Also, we would like to thank Ara Lidstrom and Ashni Vora for technical assistance, and the Moores Family Foundation, Koman Family Foundation, the Strauss Family Foundation, the Sanford Stem Cell Institute for their generous support.

References

1. Schoggins JW, Wilson SJ, Panis M, Murphy MY, Jones CT, Bieniasz P, and Rice CM (2011). A diverse range of gene products are effectors of the type I interferon antiviral response. Nature 472, 481–485. 10.1038/nature09907. [PubMed: 21478870]
2. Sánchez-Rivera FJ, Diaz BJ, Kastenhuber ER, Schmidt H, Katti A, Kennedy M, Tern V, Ho YJ, Leibold J, Paffenholz SV, et al. (2022). Base editing sensor libraries for high-throughput engineering and functional analysis of cancer-associated single nucleotide variants. Nat Biotechnol 40, 862–873. 10.1038/s41587-021-01172-3. [PubMed: 35165384]
3. Porto EM, Komor AC, Slaymaker IM, and Yeo GW (2020). Base editing: advances and therapeutic opportunities. Nat Rev Drug Discov 19, 839–859. 10.1038/s41573-020-0084-6. [PubMed: 33077937]
4. Fry LE, Peddle CF, Barnard AR, McClements ME, and MacLaren RE (2020). RNA editing as a therapeutic approach for retinal gene therapy requiring long coding sequences. Int J Mol Sci 21. 10.3390/ijms21030777.
5. Jiang Q, Isquith J, Ladel L, Mark A, Holm F, Mason C, He Y, Mondala P, Oliver I, Pham J, et al. (2021). Inflammation-driven deaminase deregulation fuels human pre-leukemia stem cell evolution. Cell Rep 34, 108670. 10.1016/j.celrep.2020.108670. [PubMed: 33503434]
6. Jiang Q, Diep R, and Jamieson C (2019). A-to-I RNA editing in leukemia stem cells - set ADAR1 on the radar. Oncotarget 10, 6047–6048. 10.18632/oncotarget.27261. [PubMed: 31692993]
7. Lazzari E, Mondala PK, Santos ND, Miller AC, Pineda G, Jiang Q, Leu H, Ali SA, Ganesan AP, Wu CN, et al. (2017). Alu-dependent RNA editing of GLI1 promotes malignant regeneration in multiple myeloma. Nat Commun 8, 1922. 10.1038/s41467-017-01890-w. [PubMed: 29203771]
8. Zipeto Maria A., Court Angela C., Sadarangani A, Delos Santos Nathaniel P., Balaian L, Chun H-J, Pineda G, Morris Sheldon R., Mason Cayla N., Geron I, et al. (2016). ADAR1 Activation Drives Leukemia Stem Cell Self-Renewal by Impairing Let-7 Biogenesis. Cell Stem Cell 19, 177–191. 10.1016/j.stem.2016.05.004. [PubMed: 27292188]
9. Jiang Q, Crews LA, Barrett CL, Chun HJ, Court AC, Isquith JM, Zipeto MA, Goff DJ, Minden M, Sadarangani A, et al. (2013). ADAR1 promotes malignant progenitor reprogramming in chronic myeloid leukemia. Proc Natl Acad Sci U S A 110, 1041–1046. 10.1073/pnas.1213021110. [PubMed: 23275297]

Author Manuscript Author Manuscript Author Manuscript Author Manuscript

10. Xu LD, and Öhman M (2018). ADAR1 Editing and its Role in Cancer. Genes (Basel) 10. 10.3390/genesl0010012.
11. Abrahamsson AE, Geron I, Gotlib J, Dao KH, Barroga CF, Newton IG, Giles FJ, Durocher J, Creusot RS, Karimi M, et al. (2009). Glycogen synthase kinase 3beta missplicing contributes to leukemia stem cell generation. Proc Natl Acad Sci U S A 106, 3925–3929. 10.1073/pnas.0900189106. [PubMed: 19237556]
12. Goff DJ, Court Recart A, Sadarangani A, Chun HJ, Barrett CL, Krajewska M, Leu H, Low-Marchelli J, Ma W, Shih AY, et al. (2013). A Pan-BCL2 inhibitor renders bone-marrow-resident human leukemia stem cells sensitive to tyrosine kinase inhibition. Cell Stem Cell 12, 316–328. 10.1016/j.stem.2012.12.011. [PubMed: 23333150]
13. Holm F, Hellqvist E, Mason CN, Ali SA, Delos-Santos N, Barrett CL, Chun HJ, Minden MD, Moore RA, Marra MA, et al. (2015). Reversion to an embryonic alternative splicing program enhances leukemia stem cell self-renewal. Proc Natl Acad Sci U S A 112, 15444–15449. 10.1073/pnas.1506943112. [PubMed: 26621726]
14. Crews LA, Balaian L, Delos Santos NP, Leu HS, Court AC, Lazzari E, Sadarangani A, Zipeto MA, La Clair JJ, Villa R, et al. (2016). RNA Splicing Modulation Selectively Impairs Leukemia Stem Cell Maintenance in Secondary Human AML. Cell Stem Cell 19, 599–612. 10.1016/j.stem.2016.08.003. [PubMed: 27570067]
15. Jiang Q, Crews LA, Holm F, and Jamieson CHM (2017). RNA editing-dependent epitranscriptome diversity in cancer stem cells. Nat Rev Cancer 17, 381–392. 10.1038/nrc.2017.23. [PubMed: 28416802]
16. Jiang Q, Isquith J, Zipeto MA, Diep RH, Pham J, Delos Santos N, Reynoso E, Chau J, Leu H, Lazzari E, et al. (2019). Hyper-Editing of Cell-Cycle Regulatory and Tumor Suppressor RNA Promotes Malignant Progenitor Propagation. Cancer Cell 35, 81–94 e87. 10.1016/j.ccell.2018.11.017. [PubMed: 30612940]
17. Hartner JC, Walkley CR, Lu J, and Orkin SH (2009). ADAR1 is essential for the maintenance of hematopoiesis and suppression of interferon signaling. Nat Immunol 10, 109–115. ni.1680 [pii] 10.1038/ni.1680. [PubMed: 19060901]
18. Lu SX, De Neef E, Thomas JD, Sabio E, Rousseau B, Gigoux M, Knorr DA, Greenbaum B, Elhanati Y, Hogg SJ, et al. (2021). Pharmacologic modulation of RNA splicing enhances anti-tumor immunity. Cell 184, 4032–4047 e4031. 10.1016/j.cell.2021.05.038. [PubMed: 34171309]
19. Ishizuka JJ, Manguso RT, Cheruiyot CK, Bi K, Panda A, Iracheta-Vellve A, Miller BC, Du PP, Yates KB, Dubrot J, et al. (2019). Loss of ADAR1 in tumours overcomes resistance to immune checkpoint blockade. Nature 565, 43–48. 10.1038/s41586-018-0768-9. [PubMed: 30559380]
20. Zhang T, Yin C, Fedorov A, Qiao L, Bao H, Beknazarov N, Wang S, Gautam A, Williams RM, Crawford JC, et al. (2022). ADAR1 masks the cancer immunotherapeutic promise of ZBP1-driven necroptosis. Nature 606, 594–602. 10.1038/s41586-022-04753-7. [PubMed: 35614224]
21. Chan TH, Lin CH, Qi L, Fei J, Li Y, Yong KJ, Liu M, Song Y, Chow RK, Ng VH, et al. (2014). A disrupted RNA editing balance mediated by ADARs (Adenosine DeAminases that act on RNA) in human hepatocellular carcinoma. Gut 63, 832–843. 10.1136/gutjnl-2012-304037. [PubMed: 23766440]
22. Qin YR, Qiao JJ, Chan TH, Zhu YH, Li FF, Liu H, Fei J, Li Y, Guan XY, and Chen L (2014). Adenosine-to-inosine RNA editing mediated by ADARs in esophageal squamous cell carcinoma. Cancer Res 74, 840–851. 10.1158/0008-5472.CAN-13-2545. [PubMed: 24302582]
23. Han L, Diao L, Yu S, Xu X, Li J, Zhang R, Yang Y, Werner HM, Eterovic AK, Yuan Y, et al. (2015). The Genomic Landscape and Clinical Relevance of A-to-I RNA Editing in Human Cancers. Cancer Cell 28, 515–528. 10.1016/j.ccell.2015.08.013. [PubMed: 26439496]
24. Lykke-Andersen S, Pinol-Roma S, and Kjems J (2007). Alternative splicing of the ADAR1 transcript in a region that functions either as a 5'-UTR or an ORF. RNA 13, 1732–1744. 10.1261/rna.567807. [PubMed: 17698644]
25. Licht K, Kapoor U, Mayrhofer E, and Jantsch MF (2016). Adenosine to Inosine editing frequency controlled by splicing efficiency. Nucleic Acids Res. 10.1093/nar/gkw325.

Author Manuscript Author Manuscript Author Manuscript Author Manuscript

26. Dharshini SAP, Taguchi YH, and Gromiha MM (2020). Identifying suitable tools for variant detection and differential gene expression using RNA-seq data. Genomics 112, 2166–2172. 10.1016/j.ygeno.2019.12.011. [PubMed: 31862361]
27. Cretu C, Agrawal AA, Cook A, Will CL, Fekkes P, Smith PG, Lührmann R, Larsen N, Buonamici S, and Pena V (2018). Structural Basis of Splicing Modulation by Antitumor Macrolide Compounds. Molecular Cell 70, 265–273.e268. 10.1016/j.molcel.2018.03.011. [PubMed: 29656923]
28. Herbert A, Wagner S, and Nickerson JA (2002). Induction of protein translation by ADAR1 within living cell nuclei is not dependent on RNA editing. Mol Cell 10, 1235–1246. S1097276502007372 [pii]. [PubMed: 12453429]
29. Fritzell K, Xu LD, Otrocka M, Andréasson C, and Öhman M (2019). Sensitive ADAR editing reporter in cancer cells enables high-throughput screening of small molecule libraries. Nucleic Acids Res 47, e22. 10.1093/nar/gky1228. [PubMed: 30590609]
30. Qian Y, Li J, Zhao S, Matthews EA, Adoff M, Zhong W, An X, Yeo M, Park C, Yang X, et al. (2022). Programmable RNA sensing for cell monitoring and manipulation. Nature 610, 713–721. 10.1038/s41586-022-05280-1. [PubMed: 36198803]
31. Stoilov P, Lin CH, Damoiseaux R, Nikolic J, and Black DL (2008). A high-throughput screening strategy identifies cardiotonic steroids as alternative splicing modulators. Proc Natl Acad Sci U S A 105, 11218–11223. 0801661105 [pii] 10.1073/pnas.0801661105. [PubMed: 18678901]
32. Teoh PJ, Chung TH, Chng PYZ, Toh SHM, and Chng WJ. (2020). IL6R-STAT3-ADAR1 (P150) interplay promotes oncogenicity in multiple myeloma with 1q21 amplification. Haematologica 105, 1391–1404. 10.3324/haematol.2019.221176. [PubMed: 31413087]
33. Kumar D, Kashyap MK, La Clair JJ, Villa R, Spaanderman I, Chien S, Rassenti LZ, Kipps TJ, Burkart MD, and Castro JE (2016). Selectivity in Small Molecule Splicing Modulation. ACS Chem Biol 11, 2716–2723. 10.1021/acschembio.6b00399. [PubMed: 27499047]
34. Chan W, La Clair J, Leon B, Trieger K, Slagt M, Verhaar M, Bachera D, Rispens M, Hofman R, de Boer V, et al. (2020). Scalable Synthesis of 17S-FD-895 Expands the Structural Understanding of Splice Modulatory Activity. Cell Reports Physical Science 100277.
35. Siegel R, Ma J, Zou Z, and Jemal A (2014). Cancer statistics, 2014. CA Cancer J Clin 64, 9–29. 10.3322/caac.21208. [PubMed: 24399786]
36. Siegel RL, Miller KD, and Jemal A (2017). Cancer Statistics, 2017. CA Cancer J Clin 67, 7–30. 10.3322/caac.21387. [PubMed: 28055103]
37. Mesa RA, Jamieson C, Bhatia R, Deininger MW, Fletcher CD, Gerds AT, Gojo I, Gotlib J, Gundabolu K, Hobbs G, et al. (2017). NCCN Guidelines Insights: Myeloproliferative Neoplasms, Version 2.2018. J Natl Compr Canc Netw 15, 1193–1207. 10.6004/jnccn.2017.0157. [PubMed: 28982745]
38. Hsu TY, Simon LM, Neill NJ, Marcotte R, Sayad A, Bland CS, Echeverria GV, Sun T, Kurley SJ, Tyagi S, et al. (2015). The spliceosome is a therapeutic vulnerability in MYC-driven cancer. Nature 525, 384–388. 10.1038/nature14985. [PubMed: 26331541]
39. Lee SC, Dvinge H, Kim E, Cho H, Micol JB, Chung YR, Durham BH, Yoshimi A, Kim YJ, Thomas M, et al. (2016). Modulation of splicing catalysis for therapeutic targeting of leukemia with mutations in genes encoding spliceosomal proteins. Nat Med. 10.1038/nm.4097.
40. Dvinge H, Kim E, Abdel-Wahab O, and Bradley RK (2016). RNA splicing factors as oncoproteins and tumour suppressors. Nat Rev Cancer 16, 413–430. 10.1038/nrc.2016.51. [PubMed: 27282250]
41. Steensma DP, Wermke M, Klimek VM, Greenberg PL, Font P, Komrokji RS, Yang J, Brunner AM, Carraway HE, Ades L, et al. (2021). Phase I First-in-Human Dose Escalation Study of the oral SF3B1 modulator H3B-8800 in myeloid neoplasms. Leukemia 35, 3542–3550. 10.1038/s41375-021-01328-9. [PubMed: 34172893]
42. Eskens FA, Ramos FJ, Burger H, O'Brien JP, Piera A, de Jonge MJ, Mizui Y, Wiemer EA, Carreras MJ, Baselga J, and Tabernero J (2013). Phase I pharmacokinetic and pharmacodynamic study of the first-in-class spliceosome inhibitor E7107 in patients with advanced solid tumors. Clin Cancer Res 19, 6296–6304. 10.1158/1078-0432.CCR-13-0485. [PubMed: 23983259]
43. Hong DS, Kurzrock R, Naing A, Wheler JJ, Falchook GS, Schiffman JS, Faulkner N, Pilat MJ, O'Brien J, and LoRusso P (2014). A phase I, open-label, single-arm, dose-escalation study of

Author Manuscript Author Manuscript Author Manuscript Author Manuscript

E7107, a precursor messenger ribonucleic acid (pre-mRNA) splicesome inhibitor administered intravenously on days 1 and 8 every 21 days to patients with solid tumors. Invest New Drugs 32, 436–444. 10.1007/s10637-013-0046-5. [PubMed: 24258465]

44. León B, Kashyap MK, Chan WC, Krug KA, Castro JE, La Clair JJ, and Burkart MD (2017). A Challenging Pie to Splice: Drugging the Spliceosome. Angew Chem Int Ed Engl 56, 12052–12063. 10.1002/anie.201701065. [PubMed: 28371109]
45. Roecklein BA, and Torok-Storb B (1995). Functionally distinct human marrow stromal cell lines immortalized by transduction with the human papilloma virus E6/E7 genes. Blood 85, 997–1005. [PubMed: 7849321]
46. Andrews S (2010). FastQC: a quality control tool for high throughput sequence data. Babraham Bioinformatics.
47. Dobin A, Davis CA, Schlesinger F, Drenkow J, Zaleski C, Jha S, Batut P, Chaisson M, and Gingeras TR (2013). STAR: ultrafast universal RNA-seq aligner. Bioinformatics 29, 15–21. 10.1093/bioinformatics/bts635. [PubMed: 23104886]
48. Li B, and Dewey CN (2011). RSEM: accurate transcript quantification from RNA-Seq data with or without a reference genome. BMC Bioinformatics 12, 323. 10.1186/1471-2105-12-323. [PubMed: 21816040]
49. Robinson MD, McCarthy DJ, and Smyth GK (2010). edgeR: a Bioconductor package for differential expression analysis of digital gene expression data. Bioinformatics 26, 139–140. 10.1093/bioinformatics/btp616. [PubMed: 19910308]
50. Ritchie ME, Phipson B, Wu D, Hu Y, Law CW, Shi W, and Smyth GK (2015). limma powers differential expression analyses for RNA-sequencing and microarray studies. Nucleic Acids Res 43, e47. 10.1093/nar/gkv007. [PubMed: 25605792]
51. Law CW, Chen Y, Shi W, and Smyth GK (2014). voom: Precision weights unlock linear model analysis tools for RNA-seq read counts. Genome Biol 15, R29. 10.1186/gb-2014-15-2-r29. [PubMed: 24485249]
52. van der Werf I, Mondala PK, Steel SK, Balaian L, Ladel L, Mason CN, Diep RH, Pham J, Cloos J, Kaspers GJL, Chan WC, Mark A, La Clair JJ, Wentworth P, Fisch KM, Crews LA, Whisenant TC, Burkart MD, Donohoe ME, Jamieson CHM. Detection and targeting of splicing deregulation in pediatric acute myeloid leukemia stem cells. Cell Rep Med. 2023 Mar 2:100962. doi: 10.1016/j.xcrm.2023.100962. Epub ahead of print. [PubMed: 36889320]
53. Crews LA, Jiang Q, Zipeto MA, Lazzari E, Court AC, Ali S, Barrett CL, Frazer KA, and Jamieson CH (2015). An RNA editing fingerprint of cancer stem cell reprogramming. J Transl Med 13, 52. 10.1186/s12967-014-0370-3. [PubMed: 25889244]
54. Bustin SA, Benes V, Garson JA, Hellemans J, Huggett J, Kubista M, Mueller R, Nolan T, Pfaffl MW, Shipley GL, et al. (2009). The MiQe guidelines: minimum information for publication of quantitative real-time PCR experiments. Clin Chem 55, 611–622. 10.1373/clinchem.2008.112797. [PubMed: 19246619]

Author Manuscript Author Manuscript Author Manuscript Author Manuscript

Highlights

- ADAR1p150 isoform-mediated A-to-I RNA editing fuels human LSC generation
- Lentiviral ADAR1 and splicing reporters enable detection of ADAR1p150 activation
- Rebecsinib inhibits ADAR1p150-driven LSC self-renewal while sparing normal HSCs
- Rebecsinib pre-IND studies show scalable chemistry and favorable pharmacokinetics

Author Manuscript Author Manuscript Author Manuscript Author Manuscript

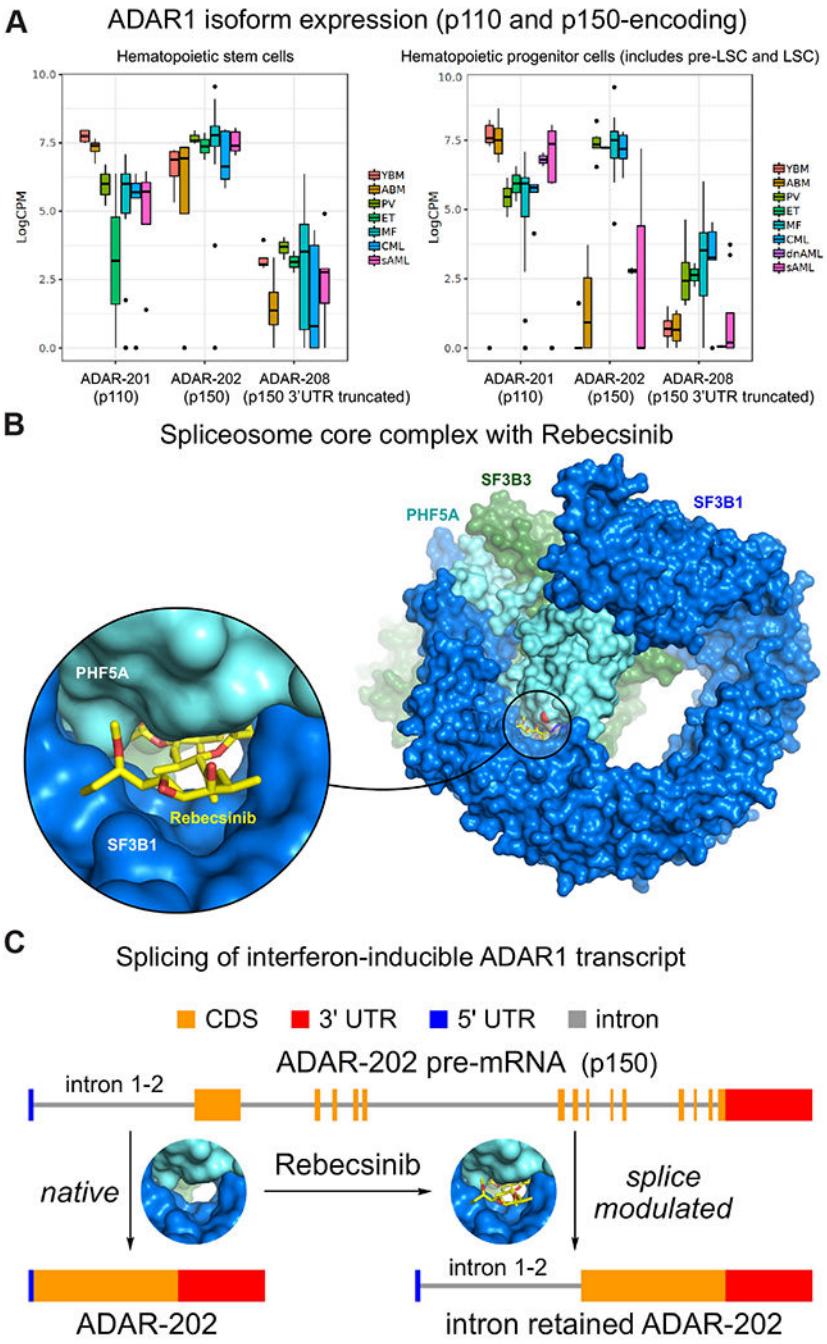

Figure 1. Quantification of ADAR1p150 by Splice Isoform RNA Sequencing (RNA-seq)

(A) RNA-seq-based quantification (counts per million, CPM) of ADAR-201 (GRCh38 ENST00000368471.8, ADAR1 p110-encoding), ADAR-202 (ENST00000368474.9, ADAR1 p150-encoding), and ADAR-208 (ENST00000529168.2, ADAR1 p150-encoding 3'UTR truncated transcripts) was performed on FACS-purified hematopoietic stem cells (HSC, $CD34^{+}CD38^{-}Lin^{-}$) from young (YBM; n=4) and aged bone marrow (ABM; n=4) HSC, polycythemia vera (PV, n=3), essential thrombocythemia (ET, n=2), myelofibrosis (MF, n=24), chronic myeloid leukemia (CML, n=5), or secondary acute myeloid leukemia

Author Manuscript Author Manuscript Author Manuscript Author Manuscript

(sAML, n=5). RNA-seq analyses were also performed on FACS-purified hematopoietic progenitor cells (HPC, $CD34^{+}CD38^{+}Lin^{-}$) from primary samples, including YBM (n=8), ABM (n=8), PV (n=6), ET (n=2), MF (n=24), CML (n=5), de novo (dnAML and sAML) (n=13) AML. Statistics for HSC: ADAR-201 $p<0.05$ for MF, CML, and sAML versus ABM; ADAR-202 $p<0.05$ for MF versus ABM; ADAR-208 differences were not significant in HSC. Statistics for HPC: ADAR-201 $p<0.05$ for PV, ET, MF, and CML versus ABM; ADAR-202 $p<0.05$ for PV, ET, MF, and CML versus ABM; ADAR-208 $p<0.05$ for PV, ET, and MF versus ABM. Statistical analyses were performed using Student's t-tests comparing MPNs and sAML versus ABM.

(B) Structural diagram showing the spliceosome core complex with Rebecsinib interacting at the interface of SF3B1 and PHF5A, adapted from the spliceosome complex bound to pladienolide B.[27]

(C) Schematic diagram of the primary ADAR1 p150-encoding transcript, *ADAR-202*, and proposed Rebecsinib-induced intron retention reducing transcript expression after treatment.

Author Manuscript Author Manuscript Author Manuscript Author Manuscript

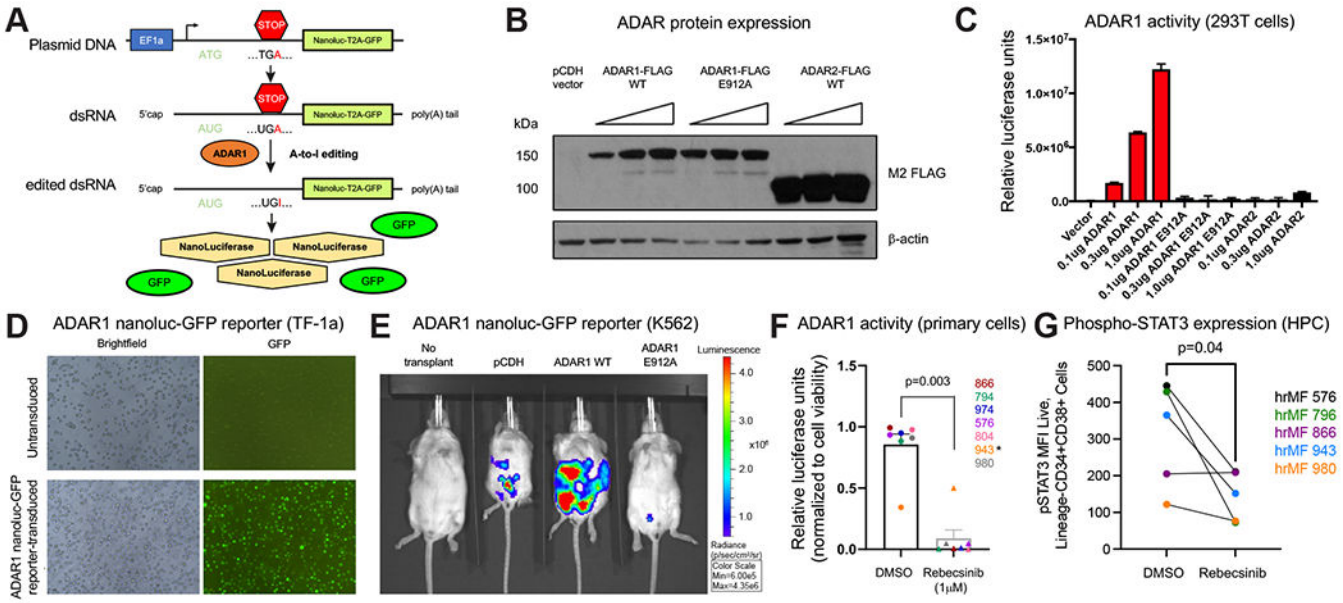

Figure 2. Development of a lentiviral ADAR1 A-to-I RNA editing reporter

(A) Schematic diagram demonstrating the synthetic RNA sequence containing an ADAR1-sensitive stop codon that, upon A-to-I editing, reads through to produce nanoluciferase and GFP proteins separated by a T2A cleavage site.

(B) ADAR protein expression levels in 293T cells co-transfected with the ADAR1 nanoluciferase-GFP (nanoluc-GFP) reporter and increasing amounts of FLAG-tagged wild-type (WT) ADAR1, catalytically inactive mutant ADAR1 (E912A), or wild-type ADAR2. β-actin was used as a loading control.

(C) Relative luciferase signals in 293T cells prepared as in panel B. Data are represented as mean ± SEM.

(D) Live cell fluorescent imaging of GFP expression in human myeloid leukemia TF-1a cells transduced with the ADAR1 nanoluc-GFP reporter vector (lower panels) compared to untransduced controls (upper panels).

(E) Detection of nanoluciferase expression via *in vivo* bioluminescence (IVIS) imaging of no transplant control (far left), K562-nanoluc-GFP and pCDH vector transduced and K562-nanoluc-GFP and ADAR1 wild-type or E912A mutant transduced human leukemia cells (K562) transplanted into RAG2$^{-/-}\gamma c^{-/-}$ mice.

(F) Luminescence-based quantification of ADAR1-dependent nanoluciferase signals in CD34^{+} cells from primary, high-risk MF samples (*=untreated patient) after *in vitro* transduction with the ADAR1 nanoluc-GFP reporter and treatment with vehicle control (DMSO) or Rebecsinib (72 hr). Relative luciferase signals were normalized to cell viability for each condition. Data are represented as mean ± SEM. $p<0.05$ compared to DMSO controls by pairwise t-test.

(G) Intracellular flow cytometry-based quantification of STAT3 phosphorylation (expressed as mean fluorescence intensity, MFI, values within HPC populations) after *in vitro* treatment with vehicle control (DMSO) or Rebecsinib (1 μM, 72 hr).

See also Figure S1.

Author Manuscript Author Manuscript Author Manuscript Author Manuscript

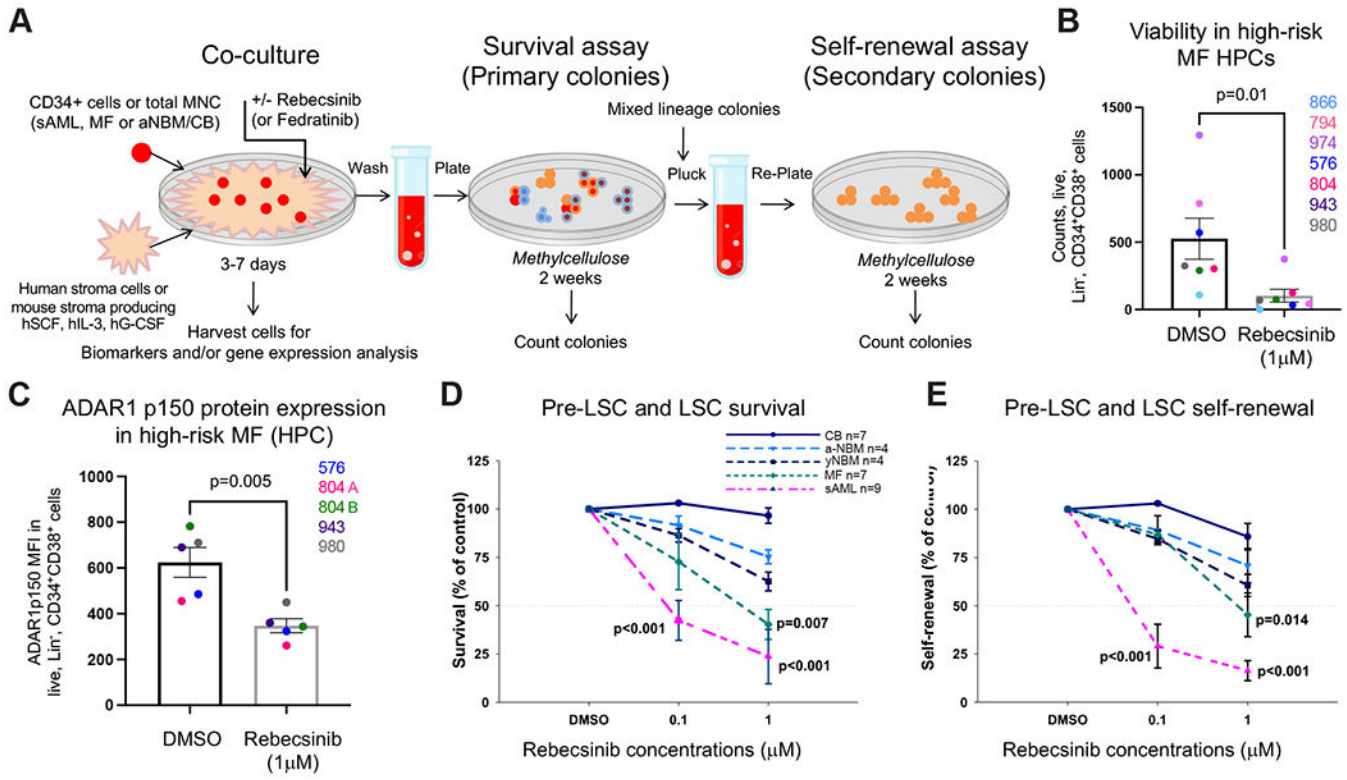

Figure 3. Rebecsinib Inhibits ADAR1p150 mediated high-risk MF HPC and LSC survival

(A) Schematic diagram of *in vitro* MF HPC and LSC survival and self-renewal assays.

(B) Flow cytometry-based viable cell counts (5,000 events measured) in high-risk MF samples after *in vitro* treatment of primary $CD34^+$ cells with vehicle control (DMSO) or Rebecsinib (72 hr).

(C) Flow cytometry-based quantification of ADAR1 p150 protein expression in high-risk MF samples after *in vitro* transduction of primary $CD34^+$ cells with ADAR1 nanoluc-GFP reporter or vector control (pCDH) followed by treatment with vehicle control (DMSO) or Rebecsinib (72 hr).

(D, E) Quantification of colony formation (survival, D) and replating (self-renewal, E) of high-risk MF HPC and sAML LSC compared with cord blood (CB) and aged versus young normal bone marrow (a-NBM, y-NBM) controls treated with Rebecsinib at increasing concentrations. Bar graphs show data as mean ± SEM and statistical analyses by pairwise t-test and dose-response assays show data as mean ± SD and statistical analyses by one-way ANOVA.

See also Figure S1.

Author Manuscript
Author Manuscript
Author Manuscript
Author Manuscript

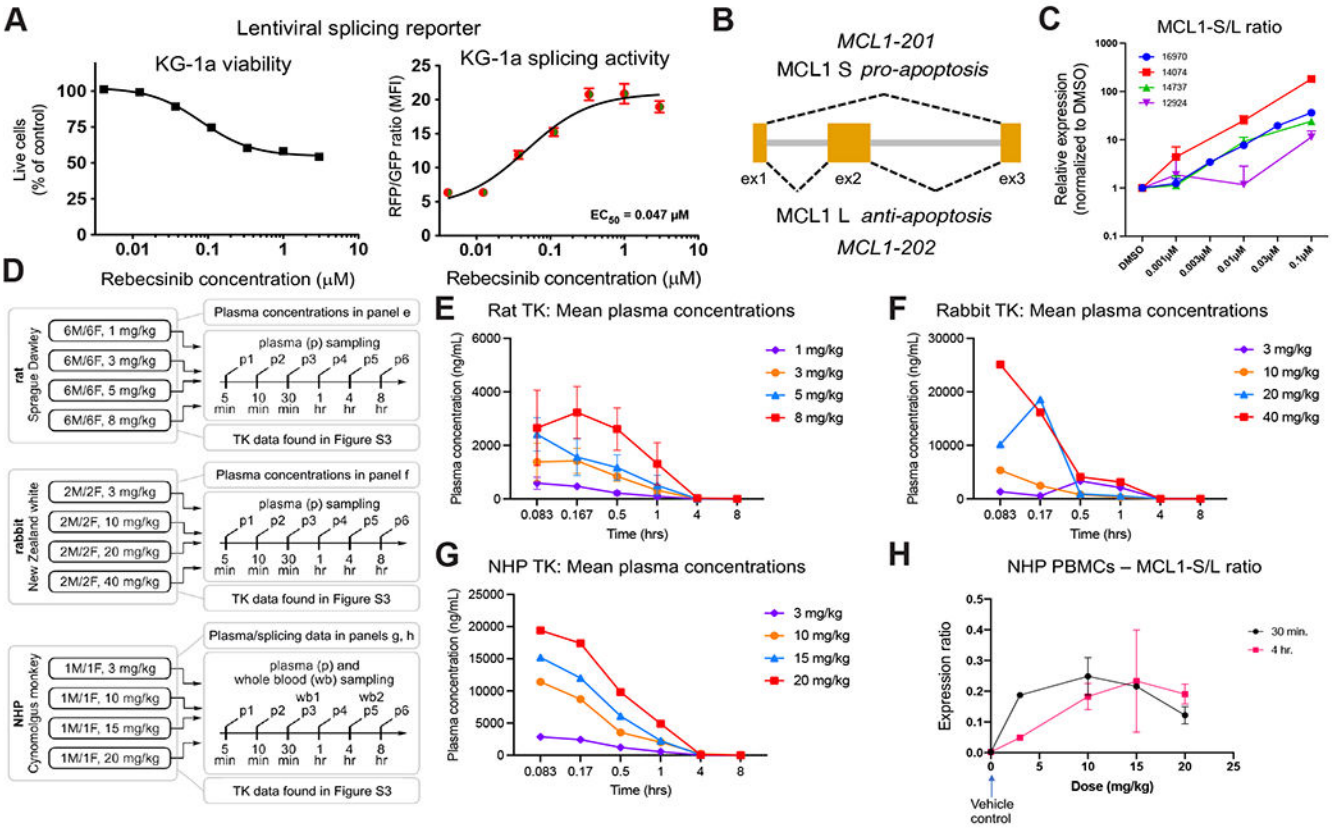

Figure 4. Rebecsinib pharmacodynamic and pharmacokinetic studies in pre-clinical and pre-IND models

(A) Quantification of cell viability (left panel) and splicing modulation (RFP/GFP ratios, right panel) by flow cytometry analyses of the human AML cell line (KG-1a) stably transduced with a lentiviral dual-fluorescence splicing reporter vector and treated with increasing concentrations of Rebecsinib.

(B) Transcript diagram illustrating alternative splicing of MCL1 to generate MCL1-short (S, pro-apoptosis) and MCL1-long (L, anti-apoptosis) variants. For human cells, the ratio of MCL1-short to long isoforms is shown.

MCL1 S/L ratios in Rebecsinib dose response assays performed using primary sAML LSC (without stromal co-culture). Splice isoform-specific qRT-PCR values were normalized to DMSO-treated controls for each individual patient sample.

(D) Schematic diagram outlining multispecies toxicokinetic (TK) and pharmacodynamic studies in mammalian species treated *in vivo* with a single dose of Rebecsinib. Toxicokinetic analyses were performed in rats (n=6 per sex, per group), rabbits (n=2 per sex, per group), and non-human primates (NHPs, n=1 per sex, per group) and pharmacodynamic splice isoform quantification studies were performed in peripheral blood mononuclear cells (PBMCs) from NHP.

(E, F) For toxicokinetic analyses, rats (E) and rabbits (F) were given a single injection of Rebecsinib at 1-40 mg/kg, or vehicle control, and blood samples were drawn at regular intervals to determine plasma concentrations of the compound over 8 hr after treatment.

Author Manuscript Author Manuscript Author Manuscript Author Manuscript

(G, H) For *in vivo* TK and complementary pharmacodynamic studies, NHPs were given a single injection of Rebecsinib at 3-20 mg/kg, or vehicle control, and blood samples were drawn at regular intervals to determine plasma concentrations (G) of the compound along with splice isoform biomarker assays to quantify MCL1 exon skipping in PBMCs isolated from treated animals (H, n=2 animals per group).

All data are represented as mean ± SEM.

See also Figures S2 and S3.

Author Manuscript Author Manuscript Author Manuscript Author Manuscript

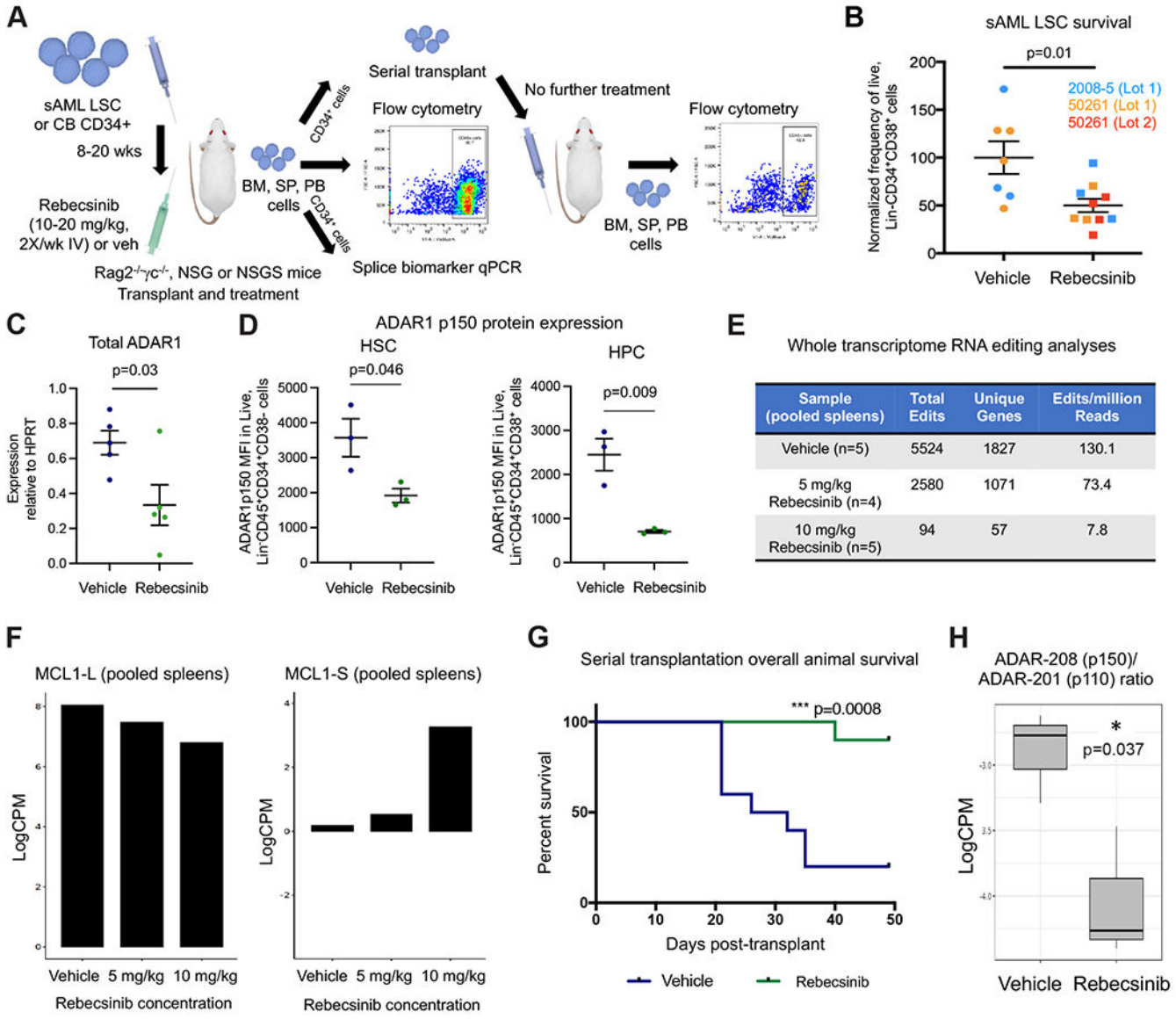

Sample (pooled spleens)	Total Edits	Unique Genes	Edits/million Reads
Vehicle (n=5)	5524	1827	130.1
5 mg/kg Rebecsinib (n=4)	2580	1071	73.4
10 mg/kg Rebecsinib (n=5)	94	57	7.8

Figure 5. ADAR1 expression and LSC self-renewal following Rebecsinib treatment

(A) Schematic diagram showing *in vivo* treatment of primary patient LSC or cord blood (CB)-engrafted mice and sAML serial transplantation studies.

(B) Flow cytometry analysis quantifying human LSC survival in sAML-engrafted mice treated with Rebecsinib Lot 1 (n=3 sAML50261, n=3 sAML 2008-5) or Lot 2 (n=4 sAML50261) compared with vehicle control (n=4 sAML50261, n=3 sAML2008-5) at 10 mg/kg twice weekly for two weeks (5 total doses).

(C) qRT-PCR analyses in CD34+ cells isolated from the spleens of sAML50261 mice treated with Rebecsinib (as in A) showing decreased total ADAR1 expression by qRT-PCR.

(D) Mean fluorescence intensity (MFI) of ADAR1p150 protein levels in human HSCs ($CD45^+CD34^+CD38^-Lin^-$) and HPCs ($CD45^+CD34^+CD38^+Lin^-$) from the spleens of sAML50261 engrafted mice treated with Rebecsinib or vehicle.

Author Manuscript Author Manuscript Author Manuscript Author Manuscript

(E) Whole transcriptome-based RNA editing analyses of previously-described RNA-seq data[14] generated from $CD34^+$ cells isolated from the spleens of sAML50261 engrafted mice treated with Rebecsinib or vehicle. Total edits, edits in unique genes, and normalized numbers of edits per million reads were calculated using RNA editing pipelines as previously described.[5]

(F) Isoform-level analysis of MCL1 transcripts from RNA-sequencing data shown in panel E.

(G) Overall mouse survival in serially transplanted sAML50261 mice (primary transplanted mice were treated with Rebecsinib or vehicle) (n=10 mice per group).

(H) Ratios of ADAR1p150-3'UTR truncated (ADAR-208) to ADAR1p110 (ADAR-201) by RNA-seq analyses of $CD34^+$ cells isolated from serial transplant recipients of sAML50261 LSC engrafted mice treated with vehicle or Rebecsinib. Serial transplant recipients received no further treatment.

Bar graphs show data as mean ± SEM and statistical analyses by unpaired t-test, and overall animal survival plot shows Kaplan-Meier plots (p=0.0008).

See also Figures S4 and S5.

Author Manuscript Author Manuscript Author Manuscript Author Manuscript

Table 1.

Demographic information including mutational status of potential disease-associated genes in MF, MPN, and sAML samples used in functional assays

Sample	Tissue	Diagnosis	Sex	Age	Blasts (% in BM)	Treatment	Number of Somatic Mutations	Notable Mutations	Cytogenetics	PDX Model Engraftment
2011-1	BM	AML	F	53	62	Idarubicin, cytarabine. Previous chemotherapy and radiation for breast cancer.	6	KIT	t(8;21)(q22;q22), cKIT+	NA
2008-5	PB	AML post-BCR-ABL-CML	M	80	61	Hydroxyurea	15	KIT, TET2, PRPF8 D1598H, SRSF2 P95S, FLT3	isochromosome 17q, trisomy 13, trisomy 19	Engrafted
50261	PB	AML post-MDS	F	72	63	None	24	DNMT3A/B, TET2, EZH2	46,XX,1,inv(3)(q21q26.2),del(5)(q14q34),der(12)t(1;12)(q21;p11.2),20,+r,+mar1[9]/46,sl,der(7)t(7;9)(p13;q13)[4]/46,sl,i(21)(q10)[3]/46,sl,add(2)(q31)[2]/46,sl,add(2)(q33)[2]	Highly engrafted
2012-17	BM	AML post-MDS	M	52	75	None	16	DNMT3A, TET2, ZRSR2	71-100,XXYY,psudic(1;17)(q32;p11.2),−5,add(5)(q13),−10,del(11)(q23),−12,−17,−17,+1-2mar,~3-28dmin[cp20]	NA
2012-8	PB	AML post-MDS	M	80	80	None	9	TP53	46-48,X,?Y,del(4)(q22q35),del5(q21q33),−7,+8,+11,+13,?del(13)(q31q33),der(15;22)(q10q10),add(17)(p13),−21,add(21)(q22),−222,+2-4mar[cp18]/48,?Y,idem,del(6)(q21),del(9)(q22q34)[cp2]	NA
2013-6	BM	AML post-MDS	F	70	15	None	16	ABL1, TP53	43-XX,add(5)(q12-13)−7,der(12)t(12;17)(p13;q12),−15,add(17)(p11.2)[2]/42-XX,add(5)(q12-13),−7,i(8)(q10),der(12)t(12;17)(p13;q12),?del(15)(q21-22),−17[5]/42-45,XX,t(1;15)(q42;q11.2),der(2)t(2;13)(p23;q12-13),add(5)(q12-13),−7,+8,t(12;17)(p13;q12),−13[12]/46,XX[3]	NA
749	PB	AML post-MF	M	77		NS-018 JAK2 inhibitor	12	JAK2 V617F	46,XY,der(7)t(1;7)(q12;q11.2)[20].nucish[EGR1,D5S23)x2[200],(D7S486x2,D7Z1x1)[185/200],(D8Z2x2)[200],(KMT2Ax2)[200],(D13S319,13qtel)x2[200]	Engrafted
14737	BM	AML post-MPN	F	28		None				NA
14074	PB	AML post-PV	M	67		Hydroxyurea, pegylated interferon,		JAK2 V617F, EVI1		NA

Author Manuscript Author Manuscript Author Manuscript Author Manuscript

Sample	Tissue	Diagnosis	Sex	Age	Blasts (% in BM)	Treatment	Number of Somatic Mutations	Notable Mutations	Cytogenetics	PDX Model Engraftment
						carbasalate calcium		overexpression		
16970	PB	AML post-PV	F	61		Ruxolitinib, hydroxyurea	7	JAK2 V617F, SRSF2 P65H, IDH2-R140, Trisomy 8		Engrafted
12924	BM	MDS-RAEB2 post-ET	M	59	88	Hydroxyurea				NA
576	PB	Myelofibrosis, high risk	F	64	<1	Pacritinib		JAK2 V617F	20q deletion	
794	PB	Myelofibrosis, high risk	F	69	1.2	Fedratinib, luspatercept		JAK2 V617F, ASXL1, VUCS: IL7R, RAD21	normal karyotype	
796	PB	Myelofibrosis, high risk	F	69	0	Ruxolitinib		CALR	duplication 1q	
804	PB	Myelofibrosis, high risk	M	82	0	Fedratinib, luspatercept, filgrastim		JAK2 V617F, DNMT3B loss, IKZF1 loss	unbalanced translocation (7;18) with loss of 7p and 18p, 20q deletion (72%)	
866	PB	Myelofibrosis, high risk	M	87	0	Ruxolitinib		JAK2 V617F, SF3B1	normal karyotype	
943	PB	Myelofibrosis, high risk	M	77		None		ASXL1 p.Q803*, SRSF2, ASXL1 p.G646fs*12		
950	PB	Myelofibrosis, high risk	M	75	1.3	Ruxolitinib		JAK2 V617F, CBL, SRSF2, SETBP1, ASXL1, VCUS: RUNX1	normal karyotype	
959	PB	Myelofibrosis, high risk	M	82		Fedratinib, allopurinol		JAK2 V617F, NRAS, TET2, SH2B3	normal karyotype	
974	PB	Myelofibrosis, high risk	M	68	0	Ruxolitinib		MPL, TET2, KMT2C, SRSF2, VUCS: MPL R.V501M, PAX5	unbalanced translocation (1;6) with 1q gain, 6p loss; loss of 20q (4%)	
980*	PB	Myelofibrosis, high risk	M	79	0	Fedratinib		TET2, ASXL1, NRAS,	normal karyotype	

Author Manuscript

Author Manuscript

Author Manuscript

Author Manuscript

Sample	Tissue	Diagnosis	Sex	Age	Blasts (% in BM)	Treatment	Number of Somatic Mutations	Notable Mutations	Cytogenetics	PDX Model Engraftment
								VCUS: EZH2		
367	BM	Normal control		53						
374	BM	Normal control		37						
388	BM	Normal control	F	67						
420	BM	Normal control	F	40						

* specimens collected on two separate days with same clinical data

Author Manuscript Author Manuscript Author Manuscript Author Manuscript

Key Resources Table

REAGENT or RESOURCE	SOURCE	IDENTIFIER
Antibodies		
CD2 (Lineage), PE-Cy5, used at 1:20	BD Pharmingen	Cat#555328
CD3 (Lineage), PE-Cy5, used at 1:20	BD Pharmingen	Cat#555334
CD4 (Lineage), PE-Cy5, used at 1:10	BD Pharmingen	Cat#555348
CD8 (Lineage), PE-Cy5, used at 1:50	BD Pharmingen	Cat#555368
CD14 (Lineage), PerCP-Cy5.5, used at 1:33	BD Pharmingen	Cat#550787
CD19 (Lineage), PE-Cy5, used at 1:50	BD Pharmingen	Cat#555414
CD20 (Lineage), PE-Cy5, used at 1:20	BD Pharmingen	Cat#555624
CD56 (Lineage), PE-Cy5, used at 1:10	BD Pharmingen	Cat#555517
CD34, APC, used at 1:50	BD Biosciences	Cat#340441
CD38, PE-Cy7, used at 1:50	BD Biosciences	Cat#335790
CD45, APC, used at 1:50	Life Technologies	Cat#MHCD4505
CD3, FITC, used at 1:20	BioLegend	Cat#300306
CD19, PE, used at 1:50	BioLegend	Cat#302208
ADAR1p150, APC, used at 1:25 (flow cytometry)	Abcam	Cat# ab269444
pSTAT3, APC, used at 1:10 (flow cytometry)	eBioscience	Cat#17-9033-42
Anti-FLAG M2	Sigma	Cat#F3165
ADAR1p150 (western blot)	Abcam	Cat#ab126745
Pan-ADAR1 (western blot)	Cell Signaling	Cat#14175 (clone D7E2M)
phospho-STAT3 (Y705) (western blot)	Cell Signaling	Cat#9145 (clone D3A7)
GAPDH	Millipore	Cat # MAB374; RRID: AB_2107445
Bacterial and virus strains		
2nd and 3rd Generation Lentiviral vectors	Core facility at UC San Diego	N/A
Biological samples		
Primary peripheral blood or bone marrow samples from patients with myeloproliferative neoplasms	Obtained through patients consented at UC San Diego according to Institutional Review Board-approved protocols Jiang et al., 2021	See Table 1
Primary young normal bone marrow	All Cells Inc, Alameda, CA	https://allcells.com
Primary aged normal bone marrow	Obtained through patients consented at UC San Diego according to Institutional Review Board-approved protocols Crews et al., 2016	See Table 1
Cord blood	All Cells Inc, Alameda, CA	https://allcells.com

Author Manuscript Author Manuscript Author Manuscript Author Manuscript

REAGENT or RESOURCE	SOURCE	IDENTIFIER
Chemicals, peptides, and recombinant proteins		
Rebecsinib (17S-FD-895)	UC San Diego Crews et al., 2016	N/A
Fedratinib	Pharmacy at Moores Cancer Center, UC San Diego	N/A
Critical commercial assays		
RNAeasy Micro Kit	Qiagen	Cat#74004
RNAeasy Mini Kit	Qiagen	Cat#74104
SuperScript III Reverse Transcriptase	ThermoFisher Scientific	Cat#18080093
SYBR GreenER qPCR SuperMix	ThermoFisher Scientific	Cat#1176202K
CD34+ MicroBead Kit, human	Miltenyi Biotec	Cat#130-046-702
Nano-Glo Luciferase Assay System	Promega	Cat#N1110
CellTiter-Glo Luciferase Assay	Promega	Cat#G7570
Live/Dead Fixable Near IR Dead Cell Stain Kit	Invitrogen	Cat#L10119
Deposited data		
Raw and analyzed primary patient sample RNA-sequencing data	Deposited at dbGaP Jiang et al., 2021	phs002228.v2
Raw and analyzed in vivo sequencing data	This paper and Crews et al., 2016	phs002228.v2
Analysis codes	This paper and Jiang et al., 2021 Archived at Zenodo (DOI: 10.5281/zenodo.7552888)	https://github.com/ucsd-ccbb/MPN_atlas_methods https://doi.org/10.5281/zenodo.7552888
Experimental models: Cell lines		
human KG-1a cells (AML cells derived from a 59 y/o male)	ATCC	CCL-246.1
human K562 cells (blast crisis chronic myeloid leukemia cells isolated from a 53 y/o female)	ATCC	CRL-3344
human TF-1a cells (erythroleukemia cells isolated from a 35 y/o male)	ATCC	CRL-2451
293T cells (human kidney epithelial cells from human fetus)	ATCC	CRL-3216
rat RBL-1 cells (leukemia cells isolated from the Wistar strain)	ATCC	CRL-1378
human MOLM-13 (sAML cells isolated from a 20 y/o male)	Provided by Dr. Dennis Carson (UC San Diego)	N/A
human HL-60 cells (acute promyelocytic leukemia cells isolated from a 36 y/o female)	ATCC	CCL-240
Experimental models: Organisms/strains		
$Rag2^{-/-}\gamma c^{-/-}$ mice, Strain #014593	Jackson Laboratories, Bar Harbor, ME	RRID:IMSR_JAX:014593
NSG-SG3M mice, Strain #013062	Jackson Laboratories, Bar Harbor, ME	RRID_IMSR JAX:013062
Sprague Dawley rats	Charles River Labs, South San Francisco, CA	N/A

Author Manuscript Author Manuscript Author Manuscript Author Manuscript

REAGENT or RESOURCE	SOURCE	IDENTIFIER
New Zealand white rabbits	BASi/Inotiv, West Lafayette, IN	N/A
cynomolgus monkeys	BASi/Inotiv	N/A
Oligonucleotides		
Primers for qRT-PCR, see Table S1	This paper	Table S1
Recombinant DNA		
ADAR1 A-to-I editing reporter	This paper	See Figure 2
pCDH-ADAR1 WT	Zipeto et al., 2016	N/A
pCDH-ADAR1^{E912A}	Zipeto et al., 2016	N/A
shADAR1-pLKO.1 (CCGGACCTCCTCACGAGCCCAAGTTCGTTTACCAAGCAAAA) (ShADAR1)	Jiang et al., 2021	N/A
shScramble -pLKO.1 (CCTAAGGTTAAGTCGCCCTCG) (ShCtrl)	Jiang et al., 2021	N/A
Dual-fluorescent lentiviral splicing reporter	This paper and Crews et al., 2016; Stoilov et al., 2008	N/A
Software and algorithms		
FlowJo	FLOWJO LLC	https://www.flowjo.com/
GraphPad Prism	GraphPad Software Inc.	https://www.graphpad.com/scientific-software/prism/
Microsoft Excel	Microsoft	
Sequencing analyses software and algorithms	This paper and Jiang et al., 2021	https://doi.org/10.5281/zenodo.7552888